Bioorganic & Medicinal Chemistry 22 (2014) 1568–1585

Contents lists available at ScienceDirect

Bioorganic & Medicinal Chemistry

journal homepage: www.elsevier.com/locate/bmc

Antiprotozoan lead discovery by aligning *dry* and *wet* screening: Prediction, synthesis, and biological assay of novel quinoxalinones

Miriam A. Martins Alho [a], Yovani Marrero-Ponce [b,d,c,*], Stephen J. Barigye [b], Alfredo Meneses-Marcel [b], Yanetsy Machado Tugores [b], Alina Montero-Torres [b], Alicia Gómez-Barrio [f], Juan J. Nogal [f], Rory N. García-Sánchez [f,h], María Celeste Vega [f,g], Miriam Rolón [f], Antonio R. Martínez-Fernández [f], José A. Escario [f], Facundo Pérez-Giménez [d], Ramón Garcia-Domenech [d], Norma Rivera [i,j], Ricardo Mondragón [i,j], Mónica Mondragón [i,j], Froylán Ibarra-Velarde [k], Atteneri Lopez-Arencibia [l], Carmen Martín-Navarro [l], Jacob Lorenzo-Morales [l], Maria Gabriela Cabrera-Serra [l], Jose Piñero [l], Jan Tytgat [e], Roberto Chicharro [m], Vicente J. Arán [n]

[a] *CIHIDECAR (CONICET), Departamento de Química Orgánica, Facultad de Ciencias Exactas y Naturales, Universidad de Buenos Aires, C1428EGA Buenos Aires, Argentina*
[b] *Unit of Computer-Aided Molecular 'Biosilico' Discovery and Bioinformatic Research (CAMD-BIR Unit), Faculty of Chemistry-Pharmacy, Universidad Central 'Marta Abreu' de Las Villas, Santa Clara 54830, Villa Clara, Cuba*
[c] *Environmental and Computational Chemistry Group, Facultad de Química Farmacéutica, Universidad de Cartagena, Cartagena de Indias, Bolivar, Colombia*
[d] *Unidad de Investigación de Diseño de Fármacos y Conectividad Molecular, Departamento de Química Física, Facultad de Farmacia, Universitat de València, Spain*
[e] *Laboratory of Toxicology, University of Leuven (KULeuven), Campus Gasthuisberg, O&N2, PO Box 922, Herestraat 49, 3000 Leuven, Belgium*
[f] *Departamento de Parasitología, Facultad de Farmacia, Universidad Complutense, 28040 Madrid, Spain*
[g] *Centro para el Desarrollo de la Investigación Científica (CEDIC), Fundación Moisés Bertoni/Díaz Gill Medicina Laboratorial, Pai Perez 1165, Asunción, Paraguay*
[h] *Laboratorio de Investigación de Productos Naturales Antiparasitarios de la Amazonía, Universidad Nacional de la Amazonía Peruana, Pasaje Los Paujiles s/n, A A.H H Nuevo San Lorenzo, San Juan Bautista, Iquitos, Peru*
[i] *Departamento de Bioquímica, Centro de Investigaciones y Estudios Avanzados del IPN, Av. Instituto Politécnico Nacional No 2508, Col. San Pedro Zacatenco, México DF 07360, Mexico*
[j] *Departamento de Microbiología y Parasitología, Facultad de Medicina, UNAM, México DF 04510, Mexico*
[k] *Department of Parasitology, Faculty of Veterinarian Medicinal and Zootecnic, UNAM, Mexico DF 04510, Mexico*
[l] *Instituto Universitario de Enfermedades Tropicales y Salud Pública de Canarias, University of La Laguna, Avda. Astrofísico Fco. Sánchez, S/N, 38203 La Laguna, Tenerife, Canary Islands, Spain*
[m] *Instituto de Química Orgánica General, CSIC, c/Juan de la Cierva 3, 28006 Madrid, Spain*
[n] *Instituto de Química Médica, CSIC, c/Juan de la Cierva 3, 28006 Madrid, Spain*

ARTICLE INFO

Article history:
Received 29 May 2012
Revised 13 January 2014
Accepted 21 January 2014
Available online 31 January 2014

Keywords:
In silico study
TOMOCOMD–CARDD software
Non-stochastic and stochastic linear indices
Classification model
Machine learning-based QSAR
Antiprotozoan database
In vitro assay
Antimalarial
Antitrypanosomal
Antitoxoplasma
Antitrichomonas
Leishmanicide
Cytotoxicity

ABSTRACT

Protozoan parasites have been one of the most significant public health problems for centuries and several human infections caused by them have massive global impact. Most of the current drugs used to treat these illnesses have been used for decades and have many limitations such as the emergence of drug resistance, severe side-effects, low-to-medium drug efficacy, administration routes, cost, etc. These drugs have been largely neglected as models for drug development because they are majorly used in countries with limited resources and as a consequence with scarce marketing possibilities. Nowadays, there is a pressing need to identify and develop new drug-based antiprotozoan therapies. In an effort to overcome this problem, the main purpose of this study is to develop a QSARs-based ensemble classifier for antiprotozoan drug-like entities from a heterogeneous compounds collection. Here, we use some of the **TOMOCOMD-CARDD** molecular descriptors and linear discriminant analysis (LDA) to derive individual linear classification functions in order to discriminate between antiprotozoan and non-antiprotozoan compounds as a way to enable the computational screening of virtual combinatorial datasets and/or drugs already approved. Firstly, we construct a wide-spectrum *benchmark* database comprising of 680 organic chemicals with great structural variability (254 of them antiprotozoan agents and 426 to drugs having other clinical uses). This series of compounds was processed by a *k*-means cluster analysis in order to design training and predicting sets. In total, seven discriminant functions were obtained, by using the whole set of atom-based linear indices. All the LDA-based QSAR models show accuracies above 85% in the training set and values of Matthews correlation coefficients (***C***) vary from 0.70 to 0.86. The external

* Corresponding author. Tel./fax: +34 963543156.
E-mail addresses: ymarrero77@yahoo.es, ymponce@gmail.com (Y. Marrero-Ponce), escario@farm.ucm.es (J.A. Escario), vjaran@iqm.csic.es (V.J. Arán).
URL: http://www.uv.es/yoma/ (Y. Marrero-Ponce).

http://dx.doi.org/10.1016/j.bmc.2014.01.036
0968-0896/

validation set shows rather-good global classifications of around 80% (92.05% for best equation). Later, we developed a multi-agent QSAR classification system, in which the individual QSAR outputs are the inputs of the aforementioned fusion approach. Finally, the fusion model was used for the identification of a novel generation of lead-like antiprotozoan compounds by using ligand-based virtual screening of 'available' small molecules (with synthetic feasibility) in our 'in-house' library. A new molecular *subsystem* (quinoxalinones) was then theoretically selected as a promising lead series, and its derivatives subsequently synthesized, structurally characterized, and experimentally assayed by using in vitro screening that took into consideration a battery of five parasite-based assays. The chemicals **11**(**12**) and **16** are the most active (*hits*) against apicomplexa (sporozoa) and mastigophora (flagellata) *subphylum* parasites, respectively. Both compounds depicted good activity in every protozoan in vitro panel and they did not show unspecific cytotoxicity on the host cells. The described technical framework seems to be a promising QSAR-classifier tool for the molecular discovery and development of novel classes of broad—antiprotozoan—spectrum drugs, which may meet the dual challenges posed by drug-resistant parasites and the rapid progression of protozoan illnesses.

1. Introduction

Diseases caused by tropical parasites affect hundreds of millions of people worldwide, mainly distributed in tropical and subtropical regions. In fact, parasitic diseases have been one of the most significant public health problems for centuries with noteworthy mortality and devastating social and economic consequences. Parasites belonging to *phylum protozoa* are the most important causal pathogens and cause several human infections with globally massive impact. For instance, malaria (*Plasmodium* spp.),[1] leishmaniasis (*Leishmania* spp.),[2] trypanosomiasis (*Trypanosoma brucei* [sleeping sickness][3] and *Trypanosoma cruzi* [Chagas disease][4]) as well as giardiasis[5]/amebiasis[6] (*Giardia lamblia*/*Entamoeba histolytica*) are among the main neglected parasitic diseases with great social impact. Trichomoniasis, one of the most common sexually transmitted diseases (with around 120 million vaginitis infections worldwide every year) caused by the flagellate protozoa *Trichomonas vaginalis*, is increasingly recognized as an important infection in women and men.[7]Other serious disease caused by a related apicomplexan parasite, *Toxoplasma gondii*, has gained increasing relevance in immunocompromised patients, such as patients with transplants, cancer, or AIDS, and in congenitally infected infants.[8]

Although most of the current anti-protozoan drugs are well known and broadly used in medical treatments, most of them are decades old and have many limitations, including the emergence of drug resistance, severe side-reactions (toxicity), low-to-medium efficacy, limitations in the routes of administration, price and other important inconveniences. These drawbacks of current antiprotozoan chemotherapy make the search for new drugs an urgent need. However, the development of such drugs has been largely neglected because they are intended for the treatment of pathologies that mainly affect poor people in regions of the world with limited resources and with scarce marketing possibilities, particularly in today's post-merger climate.

Nevertheless, the search for antiprotozoan compounds is now on the desktop of medicinal chemists and great efforts to reinvigorate the drug development pipeline for these diseases are being addressed by new consortia of scientists from the academy and industry, which are driven in large part by support from major philanthropies.[9] Recently, using whole-organism screening with compounds derived from libraries containing drugs already approved for human use (with other therapeutic use, but 'off-label' like antiparasitic efficacy), a few *hits* were identified in diversity screening assays against *T. brucei*, *Plasmodium falciparum* and *leishmania*.[10–13] In this '*trial-and-error*' search for antiprotozoan drug-like compounds a lot of chemicals had to be experimentally screened (>15,000) and the efficacy of this process was very low, yielding only 3 (and 20 additional in a second study), 19, and 40 know drugs with efficacy equal to or greater than that of the drugs used currently against leishmania-, malaria- or trypanosoma-reference (control) compounds, respectively.[10–13] In addition to the low efficiency of this type of drug discovery landscape, the usually *expensive* and *time consuming* approaches impose on us the necessity to develop alternative and more rational techniques in the classical—*trial and error*—screenings.

In order to reduce costs, pharmaceutical companies have to find new technologies in the quest of new chemical entities (NCE), where an in silico 'virtual' world of data, analysis and computer-aided molecular design can be seen as an adequate alternative to the 'real' world of synthesis and screening of compounds in the laboratory. By such means, '*the expensive commitment to actual synthesis and bioassay is made only after exploring the initial concepts with computational models and screens*'. In silico screening is now incorporated in all areas of lead discovery; from target identification and library design, to *hit* analysis and compound profiling. This theoretical(*dry*)-to-experimental(*wet*) integration procedure will be used here in order to find predictive models that permit the 'rational' identification of new antiprotozoan drug-like compounds.

1.1. Background-review of TOMOCOMD–CARDD method in drug discovery for parasitic diseases: meeting the challenge

Some of our research teams have previously reported several antimicrobial-chemoinformatic studies to drive the selection of novel chemicals as promising NCEs. In these studies, the **TOMOCOMD–CARDD** (acronym of **TO**pological **MO**lecular **COM**putational **D**esign–**C**omputer-**A**ided '**R**ational' **D**rug **D**esign) method[14] and linear discriminant analysis (LDA), have been used in order to parameterize molecules in a database and for developing classification functions, respectively. The LDA is one of most important and simple (supervised, linear and parametric) patter recognition technique that can be used to determine which variables discriminate between two or more naturally occurring groups. The **TOMOCOMD–CARDD** approach is a novel scheme the rational—in silico—molecular design and Quantitative Structure Activity/Property Relationships (QSAR/QSPR).[15–19] It calculates several new families of 2D,3D-Chiral (2.5) and 3D (geometric and topographic) non-stochastic and (simple and double) stochastic (as well as canonical forms) atom- and bond-based molecular descriptors (MDs), denominated quadratic, linear and bilinear indices in analogy to the quadratic, linear and bilinear mathematical.[15–19] For instance, the **TOMOCOMD–CARDD** strategy has been used for the in silico screening of novel molecular *subsystems* having a desired activity against *Trichomonas vaginalis*.[19–21] It was also

successfully applied to the virtual (computational) screening of novel antihelmintic compounds, which were then synthesized and evaluated in vivo on *Fasciola hepatica*.[22] Studies for the fast-track discovery of novel paramphistomicides,[17] antimalarial,[23,24] and antitrypanosomal/leishmania[4,25,26] compounds were also conducted with this theoretical method.

As result of previous studies developed by our group focused on the synthesis and activity of several families of heterocyclic betaines and salts, we have prepared many indazole,[27–30] indole,[31] cinnoline[32] and quinoxaline[33] derivatives, which have shown interesting properties as trichomonacidal,[19–21,30] antichagasic,[25,26,30] antimalarial[24] and antineoplastic[28–30] drugs.

Nowadays, the effort for the search of novel antiprotozoan drugs has increased considerably. However, do effective broad spectrum antiparasitic agents exist? Therapeutics that are efficient against most of the parasitic species are interesting (and very important) because in regions of the world where these parasites are endemic, they indeed do overlap, and several infections can occur at the same time and sometimes with similar symptoms. We initially have developed '*general*' QSAR models (based on activity datasets comprising diverse compounds corresponding to a number of mechanisms of action) to describe and predict the *individual*-antiprotozoan activity.[4,19,20,23–26,34] Nonetheless, by using this approach a different model must be used to predict *specific* antiparasitic activities for a given set of chemicals for each of the antiprotozoan species. For this reason, is important to develop a more *general* model, which includes all chemicals reported as active against any protozoan parasite. This strategy will allow us, to obtain *general* models with a broad application domain (antiprotozoan space) and maybe, to discover drug-like agents with possible broad spectrum antiparasitic activity.

In this report, we will explore the potential of **TOMOCOMD–CARDD**MDs to seek a QSARs-based ensemble classifier for antiprotozoan drug-like compounds obtained from a heterogeneous series of compounds. In the first step, we selected a wide-spectrum database of antiprotozoan drugs, which include active compounds against all kinds of protozoan parasites with diverse action modes. Next, the aforementioned MDs were calculated for this large series of active/nonactive compounds and LDA was subsequently used to fit every individual classification function. The LDA was selected as statistical technique due to its broad use and simplicity. Later on, we developed a multi-agent QSAR classification system (ensemble classifier), in which the individual QSAR outputs are the inputs for the fusion approach. Finally, the fusion model was used for the identification of a novel generation of lead-like antiprotozoans by using ligand-based virtual screening (LBVS) of smallmolecules 'available' (with synthetic feasibility) in our 'in-house' library. A new molecular *sub-system* was then theoretically selected as promising lead series, which were subsequently synthesized, structurally characterized, and experimentally assayed. Here, we also describe the original synthesis and the spectroscopic characterization of 10 molecules (new quinoxalinones) that had not been previously reported. The in vitro screening carried out here was designed by taking into account a battery of assays that included the two most representative parasites of the protozoa *subphylum*: (1) mastigophora (flagellata) and (2) apicomplexa (sporozoa). These 'parasite-based' assays are suitable for describing a rather *complete profile* of antiprotozoan activities of these new chemicals. Recently, a study based on a multi-pathogen screening strategy, integrating activity and cytotoxicity data for the selection and prioritization of lead compounds, has been reported in the literature.[35] While this approach presents a plausible advantage, particularly when experimental screening is performed on a structurally diverse data set, it is imperative that the analyzed data be obtained under homogenous experimental conditions.

2. Results and discussion

2.1. In silico studies

Three different computational experiments were developed in this study. Firstly, we present the result obtained in the construction of classification models and their assemblies by using a fusion approach (multiagent-system). Each individual model was evaluated based according to the Organization for Economic Cooperation and Development (OECD) principles.[36] Later, we describe the selection of new leads by using LBVS as well as the preparation of these new chemicals for simple and efficient methods of synthesis. Finally, the biological characterization against four different species of protozoan parasites will be presented in order to close the lead discovery cycle (experimental corroboration).

2.2. Discussion on the classification-based general QSAR for the description of antiprotozoan activity

The development of discriminant functions that allows the classification of organic-chemical drugs as active or inactive is the key step in the present approach for the discovery of new wide-spectrum antiprotozoan agents. It was therefore necessary to select a training data set of active and inactive compounds containing broad structural variability and action modes, as well as therapeutic uses.

It is well-know that the general performance and extrapolation power of the learning methods decisively depends on the selection of compounds for the training series used to build the classifier model. For this reason, and with the purpose of ensuring molecular and pharmacological diversity, we have selected a *benchmark* dataset composed by a great number of molecular entities, some of them reported as antiprotozoan[37,38] and the rest with a series of other pharmacological uses.[37,38] We consider a large database of 680 drugs having great structural variability; 254 of them are active (antiprotozoan agents) and the others are non-antiprotozoan (426 compounds having other clinical uses, such as antivirals, sedative/hypnotics, diuretics, anticonvulsivants, haemostatics, oral hypoglycemics, antihypertensives, antihelminthics, anticancer compounds and so on). The classification of these compounds as 'inactive' (without antiprotozoan activity) does not guarantee that any of these compounds present antiparasitic activities not yet detected.

Initially, two *k*-means cluster analyses (*k*-MCA) were performed for active and inactive series of chemicals, which permitted splitting the dataset into training (learning) and predicting (test) series. All cases were processed by using *k*-MCA in order to design training and predicting data series in a "rational" way. The main idea consists in carrying out a partition of either active or inactive series of chemicals in several statistically representative classes of chemicals. Thence, one may select from the members of all these classes of training and predicting series. This procedure ensures that any chemical class (as determined by the clusters derived from *k*-MCA) will be represented in both series of compounds. Then, selection of the training and prediction sets was performed by randomly selecting compounds belonging to each cluster. The training set was composed by 204 antiprotozoans and 300 inactives from a set of 680 chemicals (504, ~75%). The resting group composed of 50 actives and 126 compounds with different biological activities was prepared as a test data set for validation of the models (all molecules in the four groups as a zip file). These 176 (~25%) drugs were never used in the development of the classification models.

For these sets of compounds, two atom-based **TOMOCOMD–CARDD** MDs families (*k*th order non-stochastic $[{}^{AP}f_k\ (\bar{x})\ ]$ and stochastic $[{}^{APs}f_k\ (\bar{x})]$ linear indices) were computed.[16,22,26,34,39] These linear maps use a complete atomic properties (AP) scheme,

which characterizes a specific aspect of the atomic structure. All indices were calculated for H-atom explicit molecular graphs, that is, ${}^{AP}f_k^H(\bar{x})$ and ${}^{APs}f_k^H(\bar{x})$ for non-stochastic and stochastic linear indices, respectively. Two local (L) atom-type indices for heteroatoms (group = heteroatoms (E): E = S, N, O), not considering $[{}^{AP}f_{kL}(\bar{x}_E)]$ and considering $[{}^{AP}f_{kL}(\bar{x}_E)]$ H-atoms in the molecule, were computed as well.

All Classification-based QSAR equations were derived by using forward stepwise LDA and all the set of total and local atom-based linear computed indices are shown below:

$$\begin{aligned} Class = {} & -3.84 - 3.14 * 10^{-4M} f_5^H(\bar{x}) + 2.79 * 10^{-2M} f_1(\bar{x}) + 4.19 \\ & * 10^{-3M} f_2(\bar{x}) + 2.72 * 10^{-8M} f_{12}(\bar{x}) - 2.45 \\ & * 10^{-3M} f_{4L}^H(\bar{x}_E) + 4.23 * 10^{-6M} f_{10L}^H(\bar{x}_E) - 2.40 \\ & * 10^{-8M} f_{14L}(\bar{x}_E) \end{aligned} \quad (1)$$

$$\begin{aligned} Class = {} & -3.97 - 2.32 * 10^{-5P} f_8^H(\bar{x}) + 6.23 * 10^{-3P} f_5(\bar{x}) - 1.87 \\ & * 10^{-4P} f_9(\bar{x}) + 6.47 * 10^{-6P} f_{12}(\bar{x}) - 6.55 * 10^{-8P} f_{15}(\bar{x}) \\ & + 2.37 * 10^{-6P} f_{11L}^H(\bar{x}_E) - 1.46 * 10^{-8P} f_{15L}(\bar{x}_E) \end{aligned} \quad (2)$$

$$\begin{aligned} Class = {} & -4.03 - 1.34 * 10^{-9V} f_{14}^H(\bar{x}) + 3.37 * 10^{-3V} f_1(\bar{x}) + 8.23 \\ & * 10^{-9V} f_{13}(\bar{x}) - 2.47 * 10^{-3V} f_{4L}^H(\bar{x}_E) + 1.78 \\ & * 10^{-7V} f_{12L}^H(\bar{x}_E) + 1.84 * 10^{-2V} f_{2L}(\bar{x}_E) - 4.12 \\ & * 10^{-9V} f_{15L}(\bar{x}_E) \end{aligned} \quad (3)$$

$$\begin{aligned} Class = {} & -3.84 - 1.36 * 10^{-4K} f_8^H(\bar{x}) + 3.42 * 10^{-5K} f_9^H(\bar{x}) \\ & + 0.27^K f_0(\bar{x}) - 6.76 * 10^{-3K} f_3(\bar{x}) - 6.96 * 10^{-2K} f_{2L}^H(\bar{x}_E) \\ & + 3.76 * 10^{-5K} f_{9L}^H(\bar{x}_E) - 1.71 * 10^{-8K} f_{15L}(\bar{x}_E) \end{aligned} \quad (4)$$

$$\begin{aligned} Class = {} & -4.06 + 2.8 * 10^{-8M} f_{12}(\bar{x}) - 4.53 * 10^{-8P} f_{15L}(\bar{x}_E) \\ & + 1.34 * 10^{-7V} f_{12L}^H(\bar{x}_E) + 9.23 * 10^{-3V} f_{2L}(\bar{x}_E) - 1.36 \\ & * 10^{-5K} f_8^H(\bar{x}) + 0.14^K f_0(\bar{x}) - 6.35 * 10^{-2K} f_{2L}^H(\bar{x}_E) \end{aligned} \quad (5)$$

$$\begin{aligned} Class = {} & -3.13 - 5.28 * 10^{-2Ms} f_2^H(\bar{x}) + 0.26^{Ms} f_2(\bar{x}) \\ & - 0.18^{Ms} f_{10}(\bar{x}) + 0.10^{Ms} f_{1L}^H(\bar{x}_E) - 5.46 * 10^{-2Ms} f_{1L}(\bar{x}_E) \\ & - 0.20^{Ms} f_{2L}^H(\bar{x}_E) + 0.15^{Ms} f_{14L}(\bar{x}_E) + 3.73^{Ms} f_{3L}(\bar{x}_{H-E}) \end{aligned} \quad (6)$$

$$\begin{aligned} Class = {} & -4.00 + 0.74^{Ps} f_1^H(\bar{x}) - 0.72^{Ps} f_2^H(\bar{x}) - 0.56^{Ps} f_{11}^H(\bar{x}) \\ & + 0.87^{Ps} f_4(\bar{x}) - 2.12^{Ps} f_{1L}^H(\bar{x}_E) + 1.12^{Ps} f_{2L}^H(\bar{x}_E) \\ & + 1.31^{Ps} f_{3L}^H(\bar{x}_E) \end{aligned} \quad (7)$$

$$\begin{aligned} Class = {} & -3.79 + 0.14^{Vs} f_0^H(\bar{x}) - 0.08^{Vs} f_2^H(\bar{x}) - 0.03^{Vs} f_7^H(\bar{x}) \\ & - 0.73^{Vs} f_3^H(\bar{x}) + 1.94^{Vs} f_{5L}^H(\bar{x}_E) + 0.16^{Vs} f_{6L}^H(\bar{x}_E) \\ & - 1.30^{Vs} f_{7L}^H(\bar{x}_E) - 0.07^{Vs} f_{0L}(\bar{x}_E) \end{aligned} \quad (8)$$

$$\begin{aligned} Class = {} & -4.27 + 3.25^{Ks} f_5^H(\bar{x}) - 3.23^{Ks} f_7^H(\bar{x}) + 2.97^{Ks} f_{1L}^H(\bar{x}_E) \\ & + 3.34^{Ks} f_{6L}^H(\bar{x}_E) - 1.62^{Ks} f_{1L}(\bar{x}_E) - 4.29^{Ks} f_{6L}(\bar{x}_E) \\ & - 13.81^{Ks} f_{6L}^H(\bar{x}_{E-H}) + 60.01^{Ks} f_{10L}^H(\bar{x}_{E-H}) \\ & - 46.26^{Ks} f_{12L}^H(\bar{x}_{E-H}) \end{aligned} \quad (9)$$

$$\begin{aligned} Class = {} & -3.93 - 9.25 * 10^{-2Ms} f_{2L}(\bar{x}_E) - 0.98^{Ps} f_{1L}^H(\bar{x}_E) \\ & + 0.18^{Vs} f_{6L}^H(\bar{x}_E) + 5.98 * 10^{-2Vs} f_{0L}(\bar{x}_E) \\ & + 10.99^{Ks} f_{10L}^H(\bar{x}_{E-H}) - 11.23^{Ks} f_{12L}^H(\bar{x}_{E-H}) \end{aligned} \quad (10)$$

$$\begin{aligned} Class = {} & -3.97 - 1.89 * 10^{-3M} f_{4L}^H(\bar{x}_E) + 2.59 * 10^{-2V} f_{2L}(\bar{x}_E) \\ & - 6.96 * 10^{-2K} f_{2L}^H(\bar{x}_E) + 9.24 * 10^{-6K} f_{9L}^H(\bar{x}_E) \\ & - 0.72^{Ps} f_{1L}^H(\bar{x}_E) + 0.10^{Vs} f_{7L}^H(\bar{x}_E) \end{aligned} \quad (11)$$

In total eleven models were obtained, the first four Eqs. (1)–(4) developed with the non-stochastic bond-based linear indices and models 6–9 obtained with the stochastic MDs. The overall performances of all the obtained models are given in Table 1, together with the Wilks' statistics (λ), the square of the Mahalanobis distances (D^2), and the Fisher ratio (F). The selected models are statistically significant at p-level <0.001. Table 1 also shows the result obtained for the Eqs. 5 and 10 in both cases (non-stochastic and stochastic molecular fingerprints) resulting in a combination of all pairs of atom weights (atomic labels). In addition, the Eq. 11 was carried out by using the entire MDs set (mixing non-stochastic and stochastic linear indices) and was the best models in the learning set (see Table 1).

As can be observed in Table 1, the fitted models **5** and **10**, resulting of the combination of weighting schemes for the non-stochastic and stochastic atom-level linear indices, respectively, as well as the Eq. 11 (mixing non-stochastic and stochastic indices) exhibit the best results. These best two equations based on both individual set of linear indices (Eqs. 5 and 10) correctly classified 91.27% of the training set, and showed values of the Matthews correlation coefficients (***C***) of 0.82. However, Eq. 5 (non-stochastic linear indices) showed more false positive rate than Eq. 10, fitted by using only stochastic MDs. Even then, the best result was obtained when all MD sets were used. The Eq. 11 showed 93.06% of global good classification and a ***C*** of 0.86. The most common parameters in medical statistics for all the models are depicted in the same Table 1. Classifications of every compound in the learning series are shown in Tables SI1 and SI2, respectively, of Supporting information (see structures as zip file). Likewise a plot of the $\Delta P\%$ (see Section 4) for the entire training set by using the best model **11**, is illustrated in Figure 1.

Another crucial problem in chemometric and QSAR studies is the definition of the Applicability Domain (AD) of a classification or regression model. '*Not even a robust, significant, and validated QSAR model can be expected to reliably predict the modeled property for the entire universe of chemicals. In fact, only the predictions for chemicals falling within this domain can be considered reliable and not extrapolations model*'.[40] The AD is a theoretical region in chemical space, defined by the model descriptors and modeled response, and thus by the nature of the chemicals in the training set, is represented in each model by specific MDs. That is to say, the AD of the QSAR model is 'the range within which it *tolerates* a new molecule'.

Figure 2 shows the Williams plot for the AD of Eq. 11. As can be noted in Figure 2, almost all chemicals used lie within this area. Actually, some chemicals have leverage (h) values much higher than the threshold but show residuals within the limits, for example in the test set, Trypan red (h = 0.371) and Dithiophos (h = 0.156). These active and inactive compounds are outside the AD of this model and these chemicals can influence model parameters. Considering this fact, we must check the effect of withdrawal of these compounds on the model performance. When we studied the new parameters of the model after removal of these chemicals we detected no significant variations. Therefore, the influence of these compounds was not critical neither for model parameters nor its performance. Consequently, their removal was not justified. In addition, Sch 18545 (antiprotozoan with h of 0.113) and Siccamid (nonantiprotozoan with h of 0.109) had higher h in the training set. However, these compounds presented residuals rather lower than the previous ones. Given that these chemicals are in

Table 1
Prediction performances and statistical parameters for LDA-based QSAR models in the training set

Eqs.	Atomic labels[a]	Matthews corr. coeff.	Accuracy 'Q_{total}' (%)	Specificity (%)	Sensitivity 'hit rate' (%)	False '+' rate (%)	Landa Wilks	D^2	F
Non-Stochastic linear indices									
1	(M)	0.72	86.71	83.41	83.82	11.33	0.49	4.28	73.36
2	(P)	0.80	90.48	91.49	84.31	5.33	0.49	4.29	73.66
3	(V)	0.79	89.88	90.05	84.31	6.33	0.493	4.24	72.75
4	(K)	0.80	90.48	91.05	84.80	5.667	0.467	4.72	80.83
General model (combining all atomic labels)									
5	(NS)	0.82	91.27	92.11	85.78	5.00	0.467	4.98	80.83
Stochastic linear indices									
6	(M)	0.70	85.71	84.02	79.90	10.33	0.60	2.73	40.83
7	(P)	0.76	88.49	88.83	81.86	7.00	0.52	3.77	64.63
8	(V)	0.79	89.68	88.38	85.78	7.67	0.52	3.74	56.02
9	(K)	0.76	88.29	87.96	82.35	7.667	0.51	3.92	52.06
General model (combining all atomic labels)									
10	(SS)	0.82	91.27	93.48	84.31	4.00	0.46	4.83	96.93
Mixing all MDs (non-stochastic and stochastic indices)									
11	(**NS–SS**)	**0.86**	**93.06**	**92.89**	**89.71**	**4.67**	**0.435**	**5.35**	**107.3**

Bold values represents the Best models.
[a] M: atomic mass, P: atomic polarizability, K: atomic Mulliken electronegativity, V: van der Waals atomic volume.[51] NS, SS and NS–SS means non-stochastic MDs, stochastic MDs and whole set of MDs, respectively.

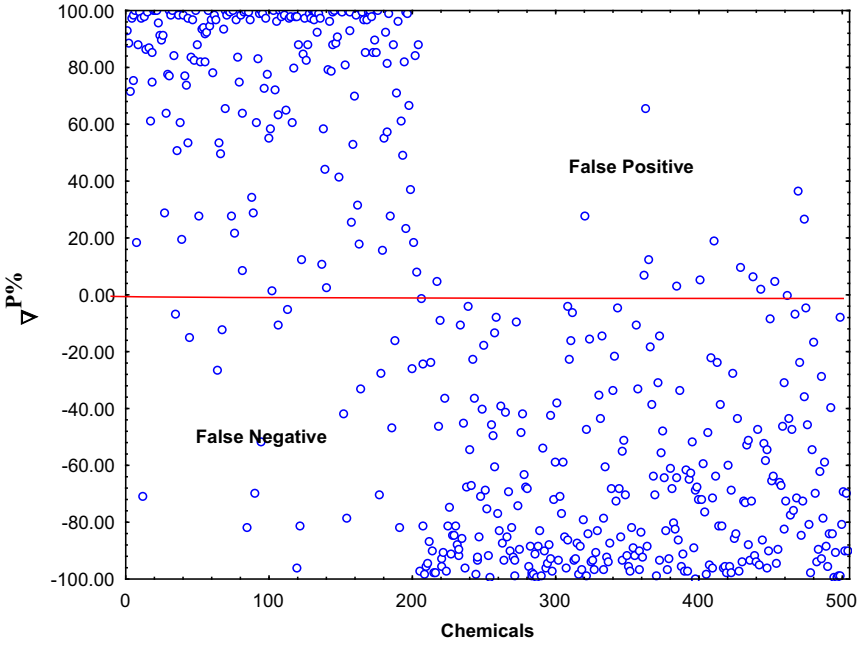

Figure 1. Plot of the $\Delta P\%$ from Eq. 11 for every compound in the training set. Compounds **1–204** and **205–504** are active and inactive, respectively.

the same experimental space as other 20 cases in the training set which slightly exceed the critical hat value (vertical line), they are slightly influential in the model development: the predictions for new compounds in this sense (for instance, included in an external test set, where there are 13 cases that slightly exceed the critical h^* value) can be considered as reliable as those of the training chemicals and the possible erroneous prediction could probably be attributed to wrong experimental data rather than to the molecular structure. Finally, two compounds Myralact (σ = 3.09) and Tosulur sodium (σ = 3.187), which are cases of training and test sets, depicted outlier behavior with standardized residuals greater than three standard deviation units. That is to say, both chemicals were wrongly predicted (>3σ); these two compounds as well as the initial two chemicals (Trypan red and Dithiophos) are completely outside the AD of the model. Thus, there are only four compounds that are either a response outlier or a high leverage chemical. Therefore, the model can be used with high accuracy in this AD. In the next section we re-take this analysis in order to determine the reliability of prediction of selected molecules as good candidates by *virtual* screening protocols.

Statistical validation of models is another key feature in good QSAR practice regarding with the diagnosis of developed models. In this sense, a QSAR model should be associated with appropriate measures of goodness-of-fit and robustness (*internal validation*), as well as predictivity (*external validation*). The evaluation of performance of models by using external validation (one or more external test sets) is viewed as a *superior alternative* because the good behavior of models in internal experiments is a necessary but not sufficient condition for the model to have high predictive power. That is, the predictivity can be claimed only if the model is successfully applied in the prediction of the external chemicals, which were not used in the model development. For this reason, in this

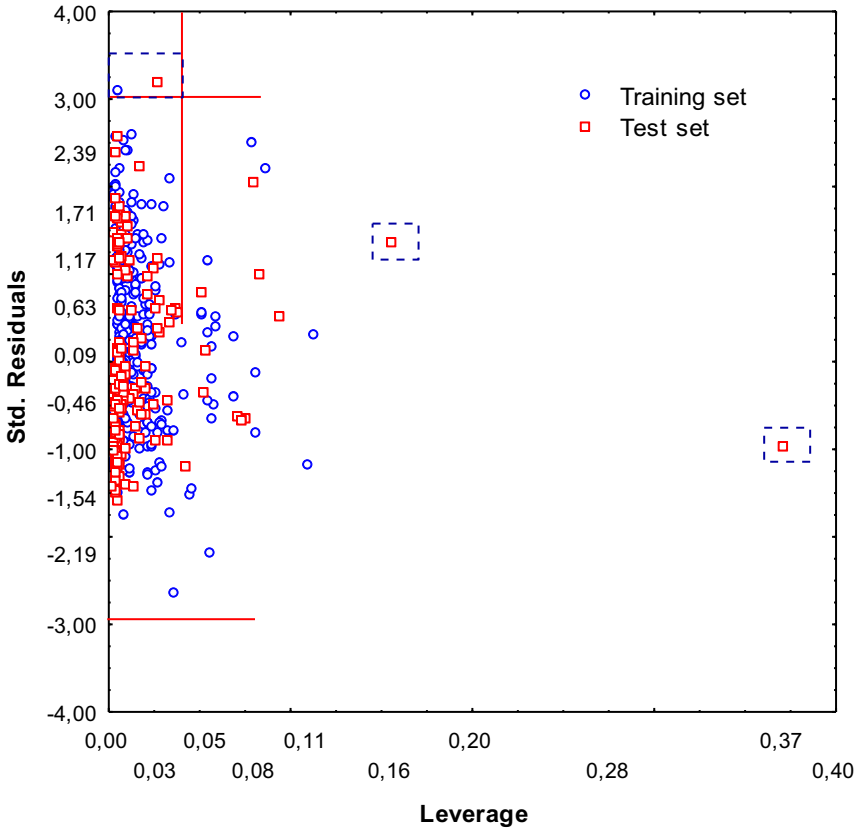

Figure 2. William plot of Eq. 11: outlier will be chemicals atpoints with standardized residuals greater than three standard deviation units; influential chemicals are points with high leverage values higher than the *threshold* or *cut-off* value $h^* = 0.042$. The training and test sets are represented by blues circles and red squares, respectively.

report we describe the external performance evaluation by using a prediction set of active and inactive compounds.

The key parameters for statistical diagnostic of all obtained models are presented in Table 2. As can be observed, the predictive performance for LDA-based QSAR models in the test set was adequate. Here, the results show that the equations obtained with non-stochastic indices are better than models derived with stochastic MDs. In addition, the best LDA-based QSAR is the Eq. 11, with an accuracy of 92.05% versus 85.80% depicted by model **5**. Finally, the classification of every compound in prediction series is illustrated as Supporting information (Tables SI3 and SI4, see structures as zip file). Likewise a plot of the $\Delta P\%$ (see Section 4) for the entire test set by using the best models **11**, is shown in Figure 3.

2.3. Drug (lead)-like discovery by virtual (in silico) screening and *dry* selection: *to be or not to be*

The ligand-based methods are supported by the principle of similarity—similar compounds are assumed to produce similar effects—and serve for modeling the complex phenomena of

Table 2
Prediction performances for LDA-based QSAR models in the test set

Eqs.	Atomic labels[a]	Matthewscorr. coeff.	Accuracy'Q_{total}' (%)	Specificity (%)	Sensitivity 'hit rate' (%)	False '+' rate (%)
Non-stochastic linear indices (NS)						
1	(M)	0.66	85.23	70.69	82.00	13.49
2	(P)	0.61	83.52	68.42	78.00	14.29
3	(V)	0.61	84.09	71.15	74.00	11.90
4	(K)	0.66	84.09	66.67	88.00	17.46
General model (combining all atomic labels)						
5	**(NS)**	0.67	85.80	71.19	84.00	13.49
Stochastic linear indices (S)						
6	(M)	0.35	71.02	49.23	64.00	26.19
7	(P)	0.41	74.43	54.24	64.00	21.43
8	(V)	0.57	81.25	63.93	78.00	17.46
9	(K)	0.42	73.30	52.17	72.00	26.19
General model (combining all atomic labels)						
10	**(SS)**	0.52	79.55	62.07	72.00	17.46
Mixing all MDs (non-stochastic and stochastic indices, NS–S)						
11	(NS–SS)	**0.81**	**92.05**	**83.33**	**90.00**	**7.14**

Bold values represents the Best models.
[a] M: atomic mass, P: atomic polarizability, K: atomic Mulliken electronegativity, V: van der Waals atomic volume.[51] NS, SS and NS–SS means non-stochastic MDs, stochastic MDs and whole set of MDs, respectively.

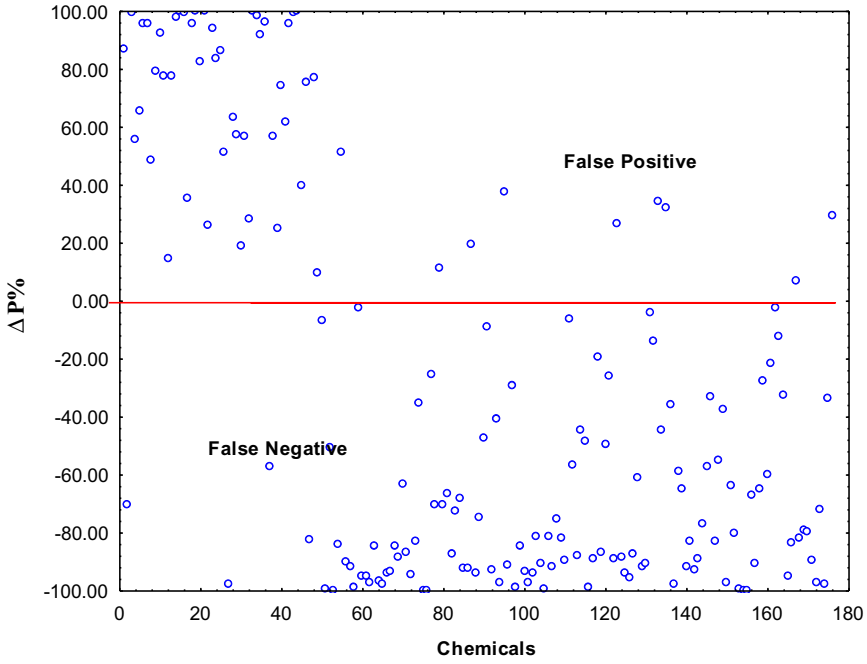

Figure 3. Plot of the Δ*P*% from Eq. 11 for every compound in the test set. Compounds **1**–**50** and **51**–**176** are active and inactive, respectively.

molecular recognition. Similarity-based methods are cornerstones of chemoinformatic and computer-aided pharmaceutical research. To this effect, LBVS has been used to identify novel active compounds in many biological applications. This indicates that 'similarity' methods should have substantial 'selectivity' in recognizing diverse active compounds. Current purposes to integrate chemoinformatics into 'real-life' applications, to step-ahead in drug discovery are of main importance nowadays.

The algorithm described above, and the obtained good results prompted us to make in silico evaluations of all the chemicals contained in our 'in-house' collections of indazole, indazolols, indole, cinnoline, and quinoxaline derivatives (as well as other new related chemicals and their derivatives), which have been recently obtained by our chemical synthesis team. On the basis of computer-aided predictions we selected potential antiprotoazoan leads (*virtual hits*). The following criteria were used for the hits selection: (1) compounds were selected as *hits* if the value of posterior probability of possessing antiprotozoan activity exceeded 15% (Δ*P* >15%) with all LDA-based QSAR models (fusion approach or multi-classification system), and (2) If, among the compounds designed (or those that would be obtained in our laboratory) by our chemical team, too many similar compounds satisfied criterion 1, then only several representative structures were selected.

Here, we performed in silico mining of our library and some heterocyclic leads were identified (selected) as novel antiprotozoan compounds by using the discriminant functions obtained through the **TOMOCOMD–CARDD** method and LDA data-mining technique as an ensemble classifier, $\mathbf{C_E}$. That is, here every individual classifier ($\mathbf{C_I}$) is fused into the $\mathbf{C_E}$ through a voting system, where the outputs of $\mathbf{C_I}$ are used as inputs for $\mathbf{C_E}$, which will have a voting *score* for the query molecules **M** (for more detail see Section 4). To provide an intuitive picture, a flowchart to show how these $\mathbf{C_I}$ are fused into the $\mathbf{C_E}$ is given in Figure 4.

One series of compounds (quinoxalinones derivatives) was selected as antiprotozoan lead-like compounds, showing good agreement between the in silico predictions and in vitro assays in several cell (parasite)-based tests (see more below). The values of Δ*P*% for this subset are depicted in Table 3.

This result shows an experimental example of QSAR application for the development of drug discovery; besides, it could be effective help for further design and optimization in this type of lead compounds as a way to improve the antiprotozoan activity, from the selection of *hits*, followed by the elucidation of the behavior in the pharmacological and toxicological assays.

However, it is generally acknowledged that QSARs are valid only within the same domain for which they were developed. In fact, even if the models are developed on the same chemicals, the AD for new chemicals can differ from model to model, depending on the specific MDs. One of the main aims of the present work was to develop a model for predicting antiprotozoan activity at early stages of drug discovery and development. Consequently, one may not pretend *to extrapolate* the use of these models to other classes of antiprotozoan activity as this would result in uncertain predictions in conditions different from those fixed to derive the model.[41,42] Therefore, the chemical designed in these studies only were synthetized and in vitro evaluated after they were found to lie in the AD of obtained models. For instance, another William plot (Fig. 5) of Eq. 11 (with the training set and quinoxalinone series discovered as novel antiprotozoan leads) was carried out. As can be noted in Figure 5, all quinoxalinones used lie within this area, which ensures great reliability for the prediction of this kind of leads used in the virtual screening.

This proves the good assessment for the classification of these quinoxalinones as novel antiprotozoan leads. Therefore, this model can be used with high accuracy for new compound predictions in this applicability domain.[41,42]

2.4. Chemistry result

Owing to their direct involvement with the present paper, special mention deserves the study performed on the synthesis and biological activity of a series of 3-alkoxy-1-[5-(dialkylamino)alkyl]-5-nitroindazoles,[30] as well as previous work on the synthesis and reactivity of quinoxalinium salts prepared from substituted acetanilides through intramolecular quaternization reactions.[33]

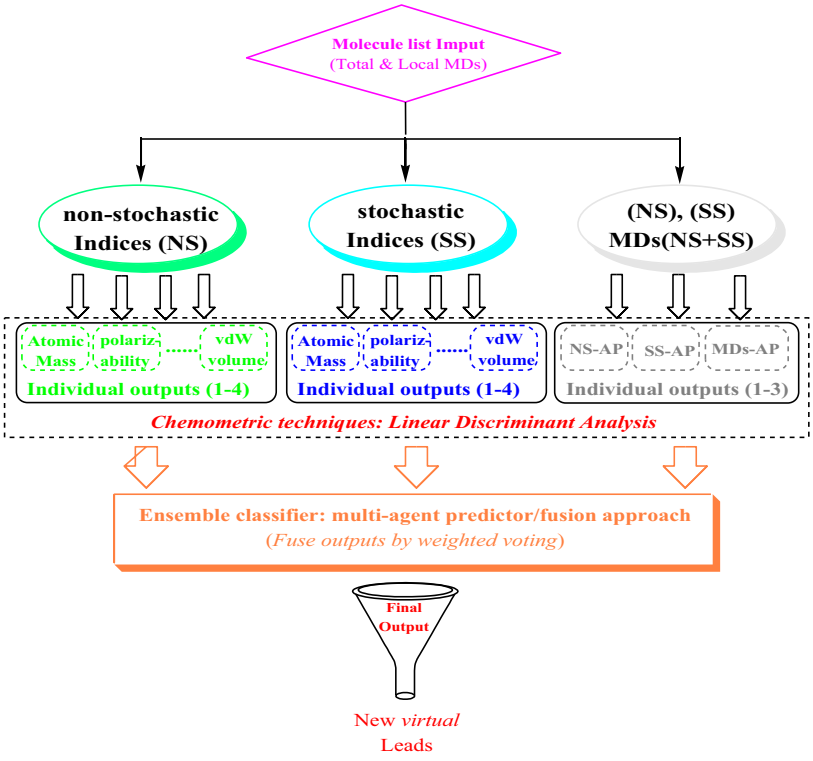

Figure 4. Flowchart illustrating how the individual classifiers are fused into the ensemble classifier through a voting system. Here we show the fusion of the discriminant functions by using **TOMOCOMD–CARDD** MDs into a prediction engine.

Table 3
Results of ligand-based in silico screening by using C_I and C_E

Compound*	Result by using whole set of C_I											C_E class[b]
	$\Delta P\%$[a] Eq. 1	$\Delta P\%$[a] Eq. 2	$\Delta P\%$[a] Eq. 3	$\Delta P\%$[a] Eq. (4	$\Delta P\%$[a] Eq. 5	$\Delta P\%$[a] Eq. 6	$\Delta P\%$[a] Eq. 7	$\Delta P\%$[a] Eq. 8	$\Delta P\%$[a] Eq. 9	$\Delta P\%$[a] Eq. 10	$\Delta P\%$[a] Eq. 11	
9	88.52	65.68	71.94	72.28	86.99	44.53	88.64	95.44	90.49	96.78	92.95	11
10	82.37	23.57	81.68	71.39	86.91	41.86	67.79	96.88	87.79	97.56	91.73	11
11	82.77	20.49	81.90	71.52	87.77	34.61	67.80	97.12	89.02	97.52	91.84	11
12	83.36	15.96	81.87	75.16	88.81	37.49	68.75	97.40	90.31	97.53	91.82	11
13	74.25	63.10	63.94	75.34	78.29	56.37	60.75	98.39	68.54	98.26	93.50	11
14	77.56	70.57	58.60	86.10	77.77	68.55	80.79	98.51	72.14	98.29	95.17	11
15	79.64	24.10	83.89	77.29	84.65	53.17	58.56	96.29	84.39	97.79	89.31	11
16	80.10	21.02	84.09	77.39	85.63	46.80	58.56	96.58	85.94	97.76	89.46	11
17	80.77	16.50	84.06	80.37	86.84	49.35	59.72	96.90	87.56	97.76	89.43	11
18	70.47	63.42	67.92	80.52	74.73	65.54	50.10	98.08	60.90	98.43	91.58	11

* The molecular structures of the compounds represented with codes (numbers) are shown in Scheme 1.

[a] $\Delta P\% = [P(\text{Active}) - P(\text{Inactive})] \times 100$ of each compounds in this screening set (see Section 4). Classification of each compounds using every obtained C_I models in the following order: Eqs. 1–11. Here, in order to consider every query molecule as active chemical we used $\Delta P\%$ >15%, because with this cut-off we avoid the not classified example as well as the risk of false active can be less.

[b] Classification of each compounds using the C_e (see Eqs. 13–17 in Section 4).

On this basis and taking into consideration the early in silico selection of the quinoxaline *molecular sub-system*as promisorial antiprotozoan lead series, we decided to prepare (synthesis and spectroscopical characterization) and evaluate the biological efficacy of 7-nitroquinoxalin-2-ones **9**–**18**, carrying at position 4 a 5-(dialkylamino)pentyl chain similar to that of the mentioned indazole derivatives, according to the synthetic pathway shown in the Scheme 1.

Thus, treatment of substituted aniline **1** with bromoacetyl bromide yielded 2-bromoacetanilide **2**, which cyclized easily to the spiro quinoxalinium bromide **5**. This salt, as well as the corresponding 1-methyl analogue **6**, could also be prepared by treatment of the previously prepared[33] chlorides **3** and **4** with hydrobromic acid through a halogen exchange reaction. The piperidine ring of salts **5** and **6** was then cleaved in refluxing nitromethane to yield the corresponding 4-(5-bromopentyl)quinoxalinones**7** and **8**.

Finally, treatment of compounds **7** and **8** with the required secondary amines (dimethylamine, pyrrolidine, piperidine, homopiperidine or 1,2,3,4-tetrahydroisoquinoline) yielded the final 4-[5-(dialkylamino)pentyl]-7-nitroquinoxalin-2-ones **9**–**18**, which were isolated as the corresponding hydrobromides. The previously prepared[33] chloro analogues of **7** and **8** were rather unreactive under the conditions used in this work (see Section 4) and were not appropriate for the preparation of the desired final compounds.

The structures for all compounds have been established on the basis of their analytical and spectral data. The latter are similar to those of related 1-[5-(dialkylamino)alkyl]indazoles,[30] quinoxalines and intermediates[33] previously prepared by our research team. Thus, NMR spectra of 2-bromoacetanilide **2** show that this compound, like the corresponding chloro analogue,[33] appears in $CDCl_3$ solution as the *Z*-rotamer. On the other hand, owing to the rigidity of spiro bromides **5** and **6**, NCH_2 protons of piperidine rings are

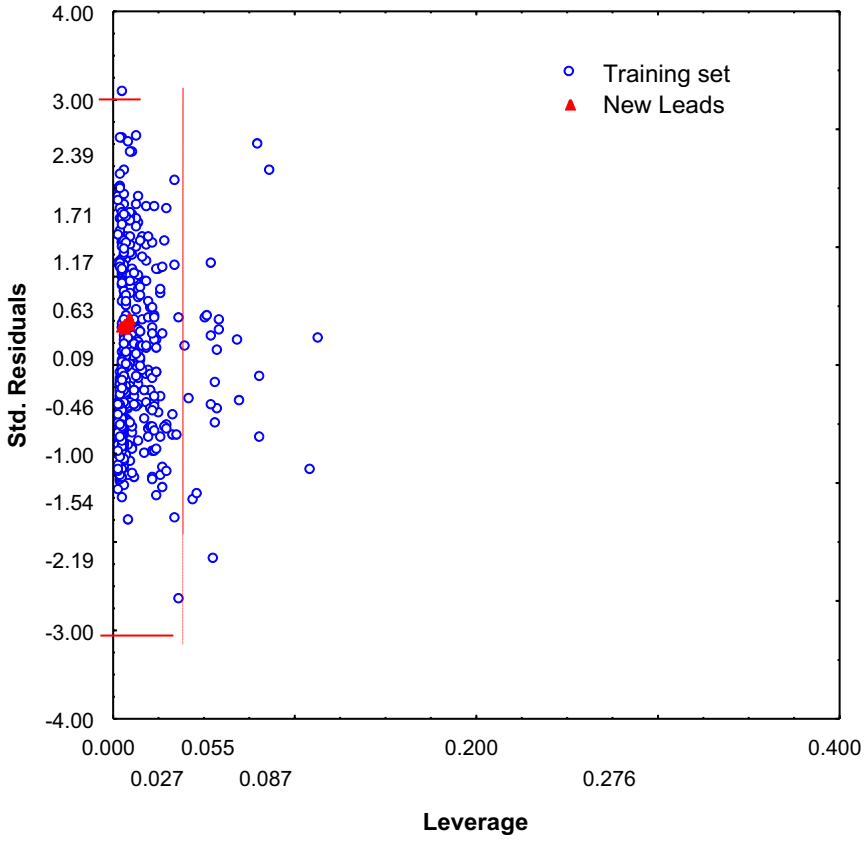

Figure 5. LDA models applicability domain for learning and new lead series. The training set is represented by blues circles and the new compounds are represented by red triangles.

anisochronic and, according to their different coupling patterns, they can be distinguished as equatorial (H_e) and axial (H_a). Similar features were observed for the cyclic secondary amine-derived final products **10**–**13** and **15**–**18**, according to their structure of tertiary ammonium bromides. The NCH_2 protons of piperidine rings of compounds **11** and **16** can also be distinguished as H_a and H_e. Nevertheless, the assignment (equatorial or axial) of other protons of the piperidine rings and protons of pyrrolidine (**10**, **15**), homopiperidine (**12**, **17**) and 1,2,3,4-tetrahydroisoquinoline (**13**, **18**) derivatives is not easy; when separate signals are observed, they have been mentioned in the description of ^{1}H NMR spectra as H_A and H_B.

2.5. In vitro screening and *wet* evaluation

In the present section we describe the main results obtained in the experimental assays (*wet evaluation*) in five different protozoan-parasite tests for the new chemicals selected as lead series in our in silico experiment. Here, we developed a *wet* screening experiment taking into account a battery of tests, that include the two most representative types of the *subphylum* protozoa parasites: (1) *T. vaginalis*, *T. cruzi* and *Leishmania braziliensis*, which belong to mastigophora (flagellata) *subphylum* and also, (2) two different apicomplexa (sporozoa) parasites: *P. falciparum* and *T. gondii*. These parasite-based tests will permit to depict a rather *complete profile* of antiprotozoan activity of these new compounds.

Firstly, we evaluate the designed compounds against *T. vaginalis* and *T. cruzi*. In the case of the latter, the epimastigote form was used in the in vitro experiment taking into consideration that this form is an obligate invertebrate (replicative form) intracellular stage. In addition, unspecific cytotoxicity to macrophages was tested for all compounds. The in vitro efficacy against *T. vaginalis* and *T. cruzi* (as well as unspecific cytotoxicity) is shown in Tables 4 and 5, respectively.

The specific activity against *T. cruzi* and *T. vaginalis* are expressed as percentages of anti-epimastigote activity and growth inhibition (cytostatic activity), respectively. The cytocidal activity (percentage of reduction with respect to the control) against *T. vaginalis* is shown in brackets. Metronidazole and Nifurtimox were used as trichomonacidal and trypanocidal reference drugs, respectively. Unspecific cytotoxic activity to macrophages is expressed as cytotoxicity percentage.

In general, all chemicals showed low unspecific cytotoxicity, except for compounds **13**, **17**, and **18** at 100 μg/mL. Most of the tested compounds, exhibited a trichomonacidals activity near to 100% (**11**–**18**, **14**) at a concentration of 100 μg/mL. Only compound **10** and **9** were inactive at this concentration. However, only chemicals **15**–**17** showed cytocidal activity against *T. vaginalis* at 10 μg/mL after 24 h of contact. These derivatives showed rather good antiprotozoan action at this level (near 90%; percentage of reduction with respect to the control), but this effect does not appear at 48 h of contact. At this time, only at the first concentration of 100 μg/mL **11**–**18** were active.

In the same form, most of the tested compounds also exhibited a trypanocidal activity of 80–100% (**10**–**13** and **16**) at 100 μg/mL. This activity was specific, since all of them, except for compound **13**, showed cytotoxicity lower than the anti-epimastigote activity (see Table 5). However, the trypanocidal activity dramatically decreases at the lowest dose. Only compound **16** retained 60% of activity at 10 μg/mL; at this concentration no cytotoxicity was shown for this compound.

In addition, we tested this series of chemicals against *L. braziliensis* which is the strain that causes a mucocutaneous form

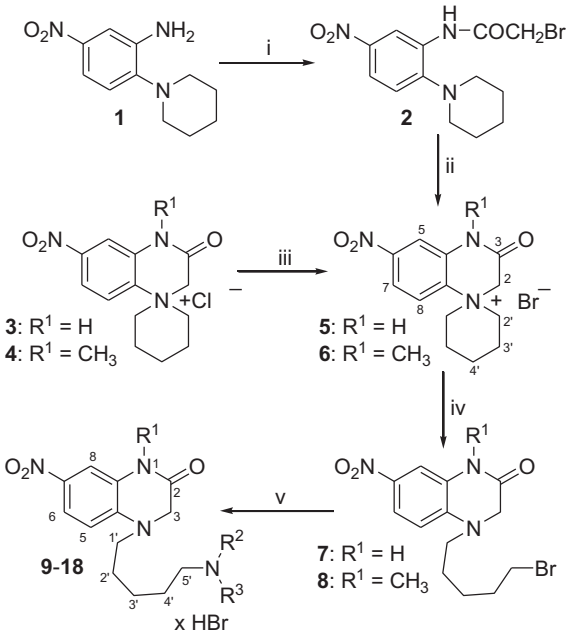

R^1 = H	R^1 = CH_3	R^2,R^3
9	**14**	CH_3,CH_3
10	**15**	$[CH_2]_4$
11	**16**	$[CH_2]_5$
12	**17**	$[CH_2]_6$
13	**18**	*o*-CH_2-C_6H_4-$[CH_2]_2$

Scheme 1. Reagents and conditions: (i) $BrCH_2COBr$, acetone, rt, 30 min; (ii) CH_3NO_2, reflux, 25 min; (iii) 48% aq HBr, vacuum evaporation to dryness (3 times); (iv) CH_3NO_2, reflux (48 h for **7** and 24 h for **8**), argon; (v) R^2R^3NH, dioxane, 100–110 °C (autoclave) or reflux, 5–10 h.

Table 4
Percentages of citostatic and/or citocidal activity [brackets] for the three concentrations assayed in vitro against *Trichomonas vaginalis*

Compound*	In vitro activity[b] (μg/mL)						
	Obs.[a]	$\%CA_{24\,h}$ [$\%C_{24\,h}$]			$\%CA_{48\,h}$ [$\%C_{48\,h}$]		
		100	10	1	100	10	1
9	–	29.39	11.43	1.22	28.33	14.68	0
10	–	75.61	21.02	3.53	34.26	1.64	0
11	+	[99.37]	20.94	0	[100]	5.74	0
12	+	[100]	12.94	2.35	[100]	0	0
13	+	[100]	83.76	3.53	[100]	44.06	0
14	+	[100]	45.71	8.98	[100]	11.26	0
15	++	[100]	[89.25]	0	[100]	67.7	4.1
16	++	[100]	[92.63]	0	[100]	86.52	0
17	++	[100]	[91.61]	10.98	[100]	70.41	2.87
18	+	[100]	70.98	4.71	[100]	23.28	4.1
Metronidazole	+++	[100]	[99.1]	[98.0]	[100]	[100]	[99.5]

* The molecular structures of the compounds represented with codes (numbers) are shown in Scheme 1.

[a] Observed (experimental activity) classification against *T. vaginalis*.

[b] Pharmacological activity of each tested compound, which was added to the cultures at doses of 100, 10 and 1 μg/mL: $\%CA_{\#}$ = Cytostatic activity$_{(24\text{ or }48\,h)}$ and [$\%C_{\#}$] = Cytocidal activity(% of reduction)$_{(24\text{ or }48\,h)}$. Metronidazole was used as positive control (concentrations for metronidazole were 2, 1 and 0.5 mg/mL, respectively).

of leishmaniasis in humans. This strain in very important because the actual clinical treatment failure, especially in patients with kala-azar, mucocutaneous leishmaniasis, and diffuse cutaneous leishmaniasis, is becoming a common problem in many areas of endemicity.[43]

Treatment of the parasites (metacyclic promastigotes) with VAM2 compounds resulted in a concentration-dependent inhibition effect on the proliferation of the tested *L. braziliensis* strain in seven of them. The compounds **17** and **15** displayed highest activity at a concentration range of 5.30 ± 0.22 > IC_{50} > 5.43 ± 0.00 μg/mL. Among the other products, the compounds **14** and **16** showed a significantly activity, IC_{50} 8.15 (±0.00) and 9.57 (±0.56) μg/mL, respectively. Among the rest of compounds evaluated, products **13**, **12** and **11** displayed an appreciable activity among promastigotesas well [IC_{50} of 31.27 (±3.16), 39.28 (±0.22) and 64.56 (±2.73) μg/mL, correspondingly]. The rest of the compounds (**9**, **10** and **18**) were inactive.

Comparing the activity against the three species of parasites (as well as cell toxicity) of these ten compounds it is possible to conclude that **15**–**17** are the best chemicals. Specifically, **16** was the most active compound in *T. cruzi* and *T. vaginalis* and also showed high activity in *L. braziliensis*. Therefore, this compound can be considered as a *hit* against mastigophora *subphylum* parasites. From these experiments, some relevant conclusions can be made about structure-activity relationship of these compounds. For instance, the methyl group at N-1 (**14**–**18**) enhances the activity against both species of flagellate protozoan parasites. The 6-member ring substituted at *N*4 (**11** and **16**) is the best chemical functional group, in contrast to the open form of this ring which was lethal during bioactivity assays (**9** and **14**) as well as when aromatic fragments were used (**13** and **18**), which also raised the toxicity observed for this lead series (see last column in Table 5).

In the second step, we evaluated the same compounds against *Toxoplasma gondii*, an important protozoon of human medical interest. Here, we initially tested the efficacy of these chemicals against the tachyzoite form of *T. gondii* (RH strain).[44,45] Tachyzoites (1×10^6) were exposed to VAM2 compounds for four hours at room temperature in order to evaluate the viability of the parasites. Five hundred tachyzoites were counted and the viability percentage was evaluated by the trypan blue exclusion method by counting the number of live tachyzoites.[44,45] Results are shown in in Table 6.

The compounds **10**–**12** showed toxoplasmicidal effects at concentrations of 500 μM and 1 mM. The VAM2-**17** was active against the parasite at 1 mM concentration. The evaluation of the parasites by light microscopy (data not shown) demonstrated that these four compounds produced the extrusion of the tachyzoites cytoplasm contents. Damage of tachyzoites with VAM2-**11** was more severe than that caused by the other three compounds. Assays were made by triplicate. Negative controls without drug treatment showed 96% viability during the assay. Compounds **13** and **18** were not evaluated because their insolubility in the cell culture MEM media.

Under these experimental approaches, we showed that some of the tested compounds have toxoplasmicidal activity mainly in the tachyzoite form. The compound **11** had the most potent anti-toxoplasma activity at high concentrations. These results suggested that the compounds **10**–**12** of this series might be considered as possible candidates in the development of toxoplasmicidal chemotherapy. More studies need to be done to evaluate the effect of the VAM2 chemicals on the structural, functional and virulent properties of *Toxoplasma gondii* in vitro and in vivo in order to design new drugs against these reemerging parasitic zoonoses. These studies are in progress and will be published in a forthcoming paper. In conclusion, compound **11**, with the same function at *N*4 as **16**, but with an H-atom in *N*1 was the most active compound. This result indicates that H-atom in the *N*1 is necessary for the anti-toxoplasma activity in contrast to that obtained in *flagellate* parasites, where the methylation of this *N*-atom was desired. The differences found in the effects of the evaluated compounds in both protozoan

Table 5
Antitrypanosomal activity and inespecific cytotoxicity at three different concentrations (100, 10 and 1 μg/mL) assayed in vitro against *Tripanosoma cruzi* and macrophagic cells, respectively

Compound*	Obs.[a]	Concentration (μg/mL)	% anti-epimastigotes[b] ± % SD	% cytotoxicity[c] ± % SD
	NT	100	NT	NT
9		10		
		1		
		100	83.54 ± 0.44	0 ± 0.55
10	+	10	5.35 ± 0.25	0 ± 2.19
		1	4.38 ± 0.30	0 ± 2.14
		100	82.4 ± 0.68	3.36 ± 1.47
11	+	10	17.68 ± 1.24	0 ± 1.51
		1	1.78 ± 8.63	0 ± 1.97
		100	97.73 ± 0.45	59.14 ± 1.77
12	+	10	23.84 ± 1.27	5.78 ± 0.58
		1	8.35 ± 5.11	0 ± 1.07
		100	87.83 ± 0.06	100 ± 0.15
13	+	10	56.77 ± 1.41	13.25 ± 0.46
		1	12.49 ± 1.85	9.89 ± 1.21
	NT	100	NT	NT
14		10		
		1		
		100	6.36 ± 4.81	49.25 ± 0.4
15	–	10	2.51 ± 5.97	0 ± 2.26
		1	0 ± 3.38	0 ± 1.25
		100	79.12 ± 3.86	61.38 ± 0.53
16	+	10	60.68 ± 2.78	11.57 ± 2.01
		1	7.93 ± 4.42	NT
		100	65.46 ± 5.47	75.75 ± 0.9
17	–	10	15.38 ± 2.83	20.24 ± 1.2
		1	0 ± 3.84	N
		100	19.78 ± 5.94	99.44 ± 0.2
18	–	10	15.62 ± 5.06	24.44 ± 0.26
		1	11.77 ± 4.35	NT
		100	98.73 ± 0.5	25.9 ± 3.9
Nifurtimox	+	10	90.0 ± 1.8	0.6 ± 3.9
		1	75.5 ± 3.9	0.0 ± 2.1

* The molecular structures of the compounds represented with codes (numbers) are shown in Scheme 1.
[a] Observed (experimental activity) classification against *T. cruzi*. Experimentally observed activity (compounds with % anti-epimastigote >70 at 100 (μg/mL) were considered as active ones).
[b] Anti-epimastigotes percentage and ±standard deviation (SD).
[c] Inespecific cytotoxicity in macrophages cells and standard deviation (SD). NT means not tested. Reference drug and positive control: Nifurtimox.

Table 6
In vitro efficacy against *Toxoplasma gondii* Tachyzoites

Compound*	Obs.[a]	% tachyzoites parasites[b]			
		1 mM	500 μM	200 μM	100 μM
9	–	73	93	96	95
10	+	0	0	85	91
11	+	0	0	68	92
12	+	0	0	82	88
13	NT	NT	NT	NT	NT
14	–	81	93	90	81
15	–	38	58	84	89
16	–	36	40	90	96
17	±	0	71	77	81
18	NT	NT	NT	NT	NT
DMSO	–	85	93	92	91

* The molecular structures of the compounds represented with codes (numbers) are shown in Scheme 1.
[a] Observed (experimental activity) against *Toxoplasma gondii* tachyzoites (RH strain).
[b] Biochemical studies of percentages of parasites (tachyzoites) for every chemicals evaluated in the range of 1 mM, 500 μM, 200 μM, 100 μM. DMSO: dimethyl sulfoxide.

subphylums might reside in the intrinsic biological properties of the mentioned parasites.

Finally, these compounds were assayed in two different tests for antimalarial screening. The first technique used was an enzymatic in vitro assay, the *so*-called: ferriprotoporphyrin IX biocrystallization inhibition test (FBIT).[46] During their digestion of host cell haemoglobin, intraerythrocytic malaria parasites produce large amounts of toxic ferriprotoporphyrin IX (FP). The inhibition of biomineralization of FP to β-hematin by some antimalarial compounds such as chloroquine underlies their action mode and in this sense, it can be used to give criteria about the antimalarial properties of such compounds.[24,46] The global results for the selected chemicals in this enzymatic in vitro model are depicted in Table 7.

From ten compounds, only 3 cases (**13**, **17** and **18**) showed activity at IC_{50} values lower than 2.0 μg/mL in the biomineralization microassay. The remaining seven, resulted inactive. In this assay, all compounds resulted less active than chloroquine (see Table 7). In terms of activity, the assayed compounds can be ordered as follows: **18** > **13** > **17**. However, these chemicals had unspecific cytotoxicity at 100 μg/mL.

Afterwards, a cell-based approach was also used to evaluate the in vitro effectivity of the designed series. This second in vitro cell-based assay was carried out by using a radioisotopic microtest in *Plasmodium falciparum* (strain 3D7).[47] Here, every compound was evaluated against cultured intraerythrocytic asexual forms of the human malaria parasite *P. falciparum*. The uptake of [G-^{3}H]hypoxanthine by parasitized erythrocytes in microtiter plates was used as an indicator of drug activity. As can be seen in Table 7, the compound **18** was also active in this *wet* evaluation, while chemicals **13** and **17** were inactive. However, compound **12** showed rather high activity in this cell assay. This compound had low cytotoxicity and was also active against *T. gondii*, therefore this chemical core and SAR result (H atom at N-1 and a 6-membered ring at N-4) can be considered as an important starting point for the design of novel

Table 7
In vitro antimalarial activity as a function of ferriprotoporphyrin IX biocrystallization inhibition test and radioisotopic microtest in *strain* 3D7 of *Plasmodium falciparum*

Compound*	Obs.[a]	Ferriprotoporphyrin IX biocrystallization inh. test IC_{50}[b] (mg/mL)	Radioisotopic microtest in strain 3D7 of *Plasmodium falciparum* IC_{50}[c] (mg/mL)
9 VAM2-9	–	>2	>10
10 VAM2-10	–	>2	>10
11 VAM2-11	–	>2	>10
12 VAM2-12	+	>2	**5.72**
13 VAM2-13	**+**	**1.53**	>10
14 VAM2-14	–	>2	>10
15 VAM2-15	–	>2	>10
16 VAM2-16	–	>2	>10
17 VAM2-17	**+**	**1.95**	>10
18 VAM2-18	**++**	**0.95**	**6.47**
Chloroquine	**++**	**0.04**	**0.04**

Bold values represents the Compound number.
* The molecular structures of the compounds represented with codes (numbers) are shown in Scheme 1.
[a] Observed (experimental activity) as a function of two different in vitro assays.
[b] IC_{50} values calculated from the percentage of inhibition obtained in ferriprotoporphyrin IX biocrystallization inhibition test (IC_{50} >2 μg/mL were considered as inactives).
[c] IC_{50} values calculated from the percentage of inhibition obtained in radioisotopic microtest in strain 3D7 of *Plasmodium falciparum* (IC_{50} >10 μg/mL were considered as inactives). Chloroquine was used as antimalarial reference drug in both assays.

anticomplexan drugs. In this sense, new refining algorithms are needed for optimizing the pharmacological, toxicological and physicochemical properties.

Additionally, all chemicals were screened for activity against *Acanthamoeba* (*Sarcodina subphylum*) and none of the compounds evaluated was active against *Acanthamoeba castellanii*. All biological details and their results are show as Supporting information (see page 24).

In summary, these results can be considered as a promising starting point for the future design and refinement of novel compounds with high anti-protozoan activity and low toxicity, although compounds **15**–**17** (lead series for anti-mastigophora *subphylum*) and **10**–**12** (lead series for anti-apicomplexan *subphylum*) were active at higher doses than their respective reference drugs. Analyzing all these in vitro results, it is clear to see that further refinement algorithms are needed to identify the ways in which the activity and ADME-Tox of the present chemical core can be optimized. Therefore, these chemicals, mainly **11**(**12**) and **16**, can be taken as *hits*, which are amenable for further chemistry optimization in order to derive products with appropriate combination of potency, pharmacokinetic properties, toxicity etc., as well as with good activity in animal models.

3. Conclusion

The integration (aligning) of *dry* and *wet* screening for diverse compounds libraries is an essential step in the quest and design of antiprotozoan lead compounds. The results of our in silico prediction and posterior in vitro screening by using a battery of parasites-cell assays are encouraging and show that such kind of methodological approaches can be successful. Within this one set of an *in house* library, we have identified 10 novel chemicals not yet reported (*virtual hits*) as antiprotozoan leads. All novel quinoxalinones were then synthetized by using simple and efficient preparations methods. The spectroscopical (structural) characterization was also presented in this report. Finally, the biological evaluation showed that most of the tested compounds, exhibited an adequate antiprotozoan activity against the four different types of parasites (*T. vaginalis, T. cruzi, L. braziliensis*, *T. gondii* and *P. falciparum*). In general, all chemicals showed low unspecific cytotoxicity, except for compounds **13**, **17**, and **18** at 100 μg/mL. However, the most active compounds, **11**(**12**) and **16**, do not present cytotoxicity in macrophages at any level. These chemicals showed preliminary evidence of efficacy and selectivity for broad antiprotozoan activity with potential for scaffold optimization.

3.1. Future perspective

The development of a new drug is a lengthy and complex process. The identification of an appropriate lead molecule is the most critical component of this phase. To this effect, here we have shown how the combination of validated QSAR-modeling and LBVS, could be successfully used as innovative technologies, to ensure high expected *hit* rates in the discovery of new bioactive compounds. In future outlooks, these models which relate the chemical structure with a specific endpoint, could be programmed into expert systems helping in exhaustive search of bioactive molecules within huge chemical libraries. That is to say, the preliminary identification of novel antiprotozoan leads in this work is promising and strongly supports the LBVS of additional compounds libraries; chemicals with diverse scaffolds must be considered in the search of new anti-parasitic compounds. In fact, the ensembleclassifier presented here will be used to identify new antiprotozoan drugs from well-known drug databases already approved for human use with potential 'off-label' antiparasitic application. The logic of this approach is that *hits* from such screens are low-hanging fruit that will require less development before they are able to enter in clinical trials as antiparasitic drugs. Some work in this direction is now under progress.

The action mode of the novel quinoxalinones described in this study is a question that has not been addressed. While this is beyond the scope of this report, it is extremely relevant, and we are currently following up on the top leads. A recent study on the action mechanisms of 7-nitroquinoxalin-2-ones as a meaning of evaluating their effectiveness against *T. cruzi* suggests as possible action mode the inhibition of the enzyme trypanothione reductase.[48] In the same spirit, we intend to explore the ADMETox properties of the screened antiprotozoan leads, as they will illuminate future studies on theiroptimization, but first explored using theoretical models. In this sense, our research group is working in the application of new 3D MDs and data mining techniques to these problems. We also intend to concentrate our efforts on the use of more sophisticated statistical techniques with the **TOMOCOMD–CARRD** MDs in order to describe the activity of organic compounds against important pharmacological *targets* of antiprotozoan drugs. Another direction to explore in future studies is the multi-optimization (approach) in order to characterize the biological response of one target chemical versus multitarget chemicals, *for instance*: different species, different molecular targets, and so on.

4. Experimental section

4.1. Computational strategies

4.1.1. Data set and classification strategy

A *benchmark* dataset usually consists of a learning (or training) dataset and an independent testing dataset. The learning dataset is one of the important components for a statistical predictor because it is used for training the predictor's 'engine', whereas the testing dataset is used for examining the predictor's accuracy via an external test. The *benchmark* dataset was composed by 680 drugs (see all structures as a zip file) having great structural variability; 254 of them are active (antiprotozoan agents) and 426 inactive compounds (drugs having other clinical uses).[37,38]

4.1.2. Representation of molecules samples

Several kinds of representations are generally used in this regard, all well-known *molecular descriptor* (MDs) or *molecular indices*. These parameters are numbers that characterize a specific aspect of the molecule structure. The *so*-called topological (and topo-chemical) indices are among the most useful MDs known nowadays. These theoretical indices are numbers that describe the structural information of molecules through graph theoretical invariants and can be considered as structure-explicit descriptors.

In the present report, a novel 2D **TOMOCOMD–CARDD** MDs family, namely atom, atom-type, and total linear indices were used in order to codify the molecular structure of every molecule in the dataset. These MDs are based on the calculation of linear maps (linear form) in $\mathscr{P}^n$ in canonical basis sets.[16,22,26,34,39] The computation of the non-stochastic and stochastic linear indices is develop by using the *k*th 'nonstochastic and stochastic graph–theoretical electronic-density matrices' $\mathbf{M}^k$and $\mathbf{S}^k$, correspondingly, as matrices of the mathematical forms.[16,22,26,34,39] These matricial operators are graph-theoretical electronic-structure models, like the 'extended Hückel MO model'. The $\mathbf{M}^1$ matrix considers all valence-bond electrons (- and π-networks) in one step, and their power k (k = 0, 1, 2, 3,...) can be considered as an interacting-electronic chemical-network in the kth step. The present approach is based on a simple model for the intramolecular (stochastic) movement of all outer-shell electrons. The theoretical scaffold of these atom-based MDs and their use to represent small-to-medium size organic chemicals, as well as QSAR and drug design studies has been explained in detail elsewhere.[16,22,26,34,39]

4.1.3. Computational methods: TOMOCOMD–CARDD approach

The **TOMOCOMD** is an interactive program for molecular design and bioinformatics research, developed upon the base of a user-friendly philosophy.[14] In this report, we only used the **CARDD** subprogram. All MDs [total and local (both atom and atom-type)] non-stochastic and stochastic linear indices were calculated in this software.

4.1.4. Chemometric studies

The statistical software package STATISTICA was used to develop the *k*-MCA.[49] The number of members in each cluster and the standard deviation of the variables in the cluster (kept as low as possible) were taken into account, to have an acceptable statistical quality of data partitions into the clusters. The values of the standard deviation between and within clusters, the respective Fisher ratio and their p level of significance, were also examined.

The LDA was also carried out with the STATISTICA software.[49] The considered tolerance parameter (proportion of variance that is unique to the respective variable) was the default value for minimum acceptable tolerance, which is 0.01. A forward-stepwise search procedure was fixed as the strategy for variable selection. The principle of parsimony (Occam's razor) was taken into account as a strategy for model selection. The quality of the models was determined by examining Wilks' λ parameter (U statistic), the square Mahalanobis distance (D^2), the Fisher ratio (F), and the corresponding p level [$p(F)$] as well as the percentage of good classification (accuracy) in the training and test sets. The classification of cases was performed by means of the posterior classification probabilities. By using the models, a compound can then be classified as active, if $\Delta P\%$ >0, being $\Delta P\%$ = [P(Active) − P(Inactive)] > 100, or as inactive otherwise. The P(Active) and P(Inactive) are the probabilities with which the equations classify a compound as active or inactive, respectively. Performing the assessment of the obtained models, the sensibility, the specificity (also known as 'hit rate'), the false positive rate (also known as 'false alarm rate'), and Matthews correlation coefficient (C), were calculated; and checked in the training and test sets.[50] Finally, the leverage approach[41]was used to evaluate the AD of the QSAR models. Through of this method it is possible to verify whether a new chemical will lie within the structural model domain. The leverage h of a compound measures its influence on the model. That is, the leverage used as a *quantitative measure* of the model AD is suitable for evaluating the degree of extrapolation, which represents a sort of compound 'distance' from the model experimental space. Prediction should be considered unreliable for compounds of high leverage values ($h > h^*$). A leverage greater than the warning leverage h^* means that the compound predicted response can be extrapolated from the model, and therefore, the predicted value must be used with great care. Only predicted data for chemicals belonging to the chemical domain of the training set should be proposed.

4.1.5. Prediction algorithms and ensemble classifier (multi-agent predictor or fusion approach)

Here, we used nonstochastic and stochastic linear indices to develop classification-based QSAR models in order to classify molecules as antiprotozoan or inactive compounds. These MDs have a few parameters that can be 'modified' in the calculation process. The number of these *uncertain* parameters depends on the atom-labels (AP scheme) used for the prediction engine. It would be much more tedious and time-consuming to determine the optimal values for AP [AP:[51] atomic mass (AP = M), atomic polarizability (AP = P), atomic Mulliken electronegativity (AP = K) and van der Waals atomic volume (AP = V)]. In addition, the number of uncertain parameters also depends on which MDs sets are used to represent the chemical samples. For instance, here every model can be fitted by two kinds of MD sets: (1) non-stochastic MDs (NS), (2) stochastic MDs (SS). To solve the problem, we use a [2AP + 1NS + 1SS + 1(NS + SS)]-dimensional *fusion approach* (11 models in total), similar to that done in protein research.

First, the basic individual classifiers to be generally expressed as$\mathbf{C_I}$(NS − AP, SS − AP, NS, SS, NS + SS)andthe predicted classification results for a query molecule **M** by each of the individual classifiers can be formulated by,

$$\mathbf{C_I}(\mathrm{NS-AP, SS-AP, NS, SS, NS+SS})\rangle\mathbf{M} = \mathbf{C}_{\mathrm{NS-AP,SS-AP,NS,SS,NS+SS}}(\mathbf{M}) \in \mathbf{S} \quad (12)$$

where, the symbol › is an action operator meaning using $\mathbf{C_I}$(NS − AP, SS − AP, NS, SS, NS + SS) to classify **M**, **S** representing the union of the two subsets defined (active or inactive). Therefore, the final predicted result should be determined by a fusion approach through the following *voting mechanism*. Now let us introduce an ensemble classifier $\mathbf{C_E}$, which is formed by fusing all set of the basic individual classifiers $\mathbf{C_I}$(NS − AP, SS − AP, NS, SS, NS + SS) and can be formulated as follows:

$$\mathbf{C_E} = \mathbf{C_1}(\mathbf{M},\mathbf{NS}) \forall \mathbf{C_2}(\mathbf{K},\mathbf{NS}) \forall \mathbf{C_3}(\mathbf{P},\mathbf{NS}) \forall \mathbf{C_4}(\mathbf{V},\mathbf{NS}) \forall \mathbf{C_5}(\mathbf{all\ AP},\mathbf{NS}) \ldots \forall \mathbf{C_6}(\mathbf{M},\mathbf{SS}) \forall \mathbf{C_7}(\mathbf{K},\mathbf{SS}) \forall \mathbf{C_8}(\mathbf{P},\mathbf{SS}) \forall \mathbf{C_9}(\mathbf{V},\mathbf{SS}) \forall \mathbf{C_{10}}(\mathbf{all\ AP},\mathbf{SS}) \ldots \forall \mathbf{C_{11}}(\mathbf{all\ AP},\mathbf{NS}+\mathbf{SS}) \quad (13)$$

where the symbol ∀ denotes the fusing operator. Then, the voting *score* for the query molecules **M** belonging to the *c*th class is given by,

$$\pi_c = \sum_{\mathrm{AP}=1}^{4} \sum_{\mathrm{MDs}=1}^{2} w_{\mathrm{AP,MDs}} \Delta(\mathrm{AP,MDs},S_c) + \sum_{\mathrm{MDs}=1}^{3} w_{\mathrm{all-AP,MDs}} \Delta(\mathrm{all-AP,MDs},S_c), (c=1,-1) \quad (14)$$

where, $S_c = 1$ is for antiprotozoans and $S_c = -1$ for non-antiprotozoans, $w_{\mathrm{AP,MDs}}$ and $w_{\mathrm{all\text{-}AP,MDs}}$ are the *weight factors* and were set at 1 for simplicity. The delta functions in Eq. 14 is given by,

$$\Delta(\mathrm{AP,MDs},S_c) = \begin{cases} 1 & \text{if } C_{\mathrm{AP,MDs}}(M) \in S_c \\ 0 & \text{otherwise} \end{cases} \quad (15)$$

$$\Delta(\mathrm{all-AP,MDs},S_c) = \begin{cases} 1 & \text{if } C_{P,\mathrm{MDs}}(M) \in S_c \\ 0 & \text{otherwise} \end{cases} \quad (16)$$

thus the query Molecule **M** is predicted belonging to the class (*c*) or subset **S***c* for which the score of Eq. 14 is the highest; that is,

$$\mu = \arg\max_c \{\pi_c\} \quad (c=1,-1) \quad (17)$$

where, μ is the argument of *c* that maximizes π_c. If there is a tie, then the final predicted result will be randomly assigned (or is take as unclassified) to one of the corresponding subsets although this kind of tie case rarely happens and was actually not observed in the current study.

4.2. Chemistry

4.2.1. Instrumental data

Mps were determined in a Stuart Scientific melting point apparatus SMP3. The mps of quinoxalinium salts **5** and **6,** as well as those of some of the final products (hydrobromides **9**–**18**) are not very well defined; these compounds decompose on heating and the observed mps are frequently heating-rate dependent and previous softening is usual. ^{1}H (300 or 400 MHz) and ^{13}C (75 or 100 MHz) NMR spectra were recorded on Varian Unity 300 or Varian Inova 400 spectrometers. The chemical shifts are reported in ppm from TMS (δ scale) but were measured against the solvent signal. The *J* values are given in Hz. The assignments have been performed by means of different standard 1D and 2D correlation experiments (NOE, COSY, HMQC and HMBC). The numbering used in the description of NMR spectra of spiro compounds **5** and **6**, and 4-substituted quinoxalinones **7**–**18** is shown in Scheme 1; double primed numbers refer to the cyclic secondary amine rings of final compounds **9**–**18**. The electron impact (EI) and electrospray (ES) mass spectra were obtained at 70 eV on a Hewlett Packard 5973 MSD spectrometer or on a Hewlett Packard 1100 MSD spectrometer, respectively. DC-Alufolien silica gel 60 PF_{254} (Merck, layer thickness 0.2 mm) was used for TLC. Microanalyses were performed by the department of Analysis, Center of Organic Chemistry 'Manuel Lora Tamayo' CSIC, Madrid, Spain.

4.2.2. Procedure for the preparation of all chemicals

4.2.2.1. 2-Bromo-5′-nitro-2′-piperidinoacetanilide (2) Bromoacetyl bromide (9.08 g, 45 mmol) was dropped (ca. 5 min) into a solution of 5-nitro-2-piperidinoaniline (**1**)[27] (8.85 g, 40 mmol) in acetone (150 mL). After 15 min, an additional amount of bromoacetyl bromide (ca. 1 mL) was dropped and the mixture stirred for 15 min. The obtained suspension (**2** × HBr) was poured into water (1 L), and the mixture stirred for 30 min. The solid in suspension, collected by filtration, washed with water (4 × 100 mL) and air-dried was shown to be bromoacetanilide **2** (13.28 g, 97% yield). This compound, crystallized from ethanol, melts partially and resolidifies at 123–125 °C (decomposition to spiro salt **5**, TLC), showing a further mp at 186–190 °C (corresponding to that of salt **5**, see below); ^{1}H NMR ($CDCl_3$): δ 9.40 (s, 1H, NH), 9.20 (d, *J* = 2.7 Hz, 1H, 6′-H), 7.97 (dd, *J* = 8.8, 2.7 Hz,1H, 4′-H), 7.21 (d, *J* = 8.8 Hz, 1H, 3′-H), 4.09 (s, 2H, 2-H), 2.87 (m, 4H, 2″-,6″-H), 1.81 (m, 4H, 3″-,5″-H), 1.62 (m, 2H, 4″-H); ^{13}C NMR ($CDCl_3$): δ 163.46 (C-1), 148.95 (C-2′), 144.16 (C-5′), 132.65 (C-1′), 120.31, 120.01 (C-3′, -4′), 114.47 (C-6′), 53.32 (C-2″, -6″), 29.59 (C-2), 26.35 (C-3″, -5″), 23.75 (C-4″); MS (EI): *m*/*z* (%) 343 (12) ([M+2]$^+$), 341 (12) (M$^+$), 262 (85), 220 (100), 203 (35), 192 (13), 174 (25), 164 (16), 145 (10), 118 (19). Anal. Calcd for $C_{13}H_{16}BrN_3O_3$ (342.19): C 45.63; H 4.71; N 12.28. Found: C 45.70; H 4.67; N 12.12.

4.2.2.2. 6-Nitro-3-oxo-1,2,3,4-tetrahydroquinoxaline-1-spiro-1′-piperidinium bromide (5). *(a) From bromoacetanilide **2***: A solution of anilide **2** (0.68 g, 2.0 mmol) in nitromethane (10 mL) was refluxed for 25 min. After cooling, the insoluble bromide **5** (0.59 g, 87% yield) was collected by filtration, washed with acetone (3 × 10 mL) and air-dried. *(b) From tetrahydroquinoxaline-1-spiro-1′-piperidinium chloride **3***: Chloride **3** (prepared[33] by cyclization of 2-chloro analogue of **2**) (7.44 g, 25 mmol) was dissolved in 48% aq hydrobromic acid and evaporated to dryness. This process was repeated twice and, after addition of acetone (100 mL), the insoluble salt **5** (8.47 g, 99% yield) was collected by filtration, washed with acetone (3 × 40 mL) and air-dried. Mp 187–192 °C (decomp.) (water); ^{1}H NMR (DMSO-d_6): δ 11.88 (s, 1H, 4-H), 8.30 (d, *J* = 9.0 Hz, 1H, 8-H), 8.13 (dd, *J* = 9.0, 2.6 Hz,1H, 7-H), 8.01 (d, *J* = 2.6 Hz, 1H, 5-H), 4.89 (s, 2H, 2-H), 4.12 (m, J_{gem} = (−)12.0 Hz, $J_{a,a}$ = 9.6 Hz, 2H, 2′-,6′-H$_a$), 3.84(br d, J_{gem} = (−)12.0 Hz, 2H, 2′-,6′-H$_e$), 2.18 (m, 2H) and 1.98-1.50 (m, 4H) (3′-,4′-,5′-H); ^{13}C NMR (DMSO-d_6): δ 160.74 (C-3), 148.59 (C-6), 134.98, 133.47 (C-4a, -8a), 122.84 (C-8), 118.38 (C-7), 112.89 (C-5), 61.72 (C-2′, -6′), 55.05 (C-2), 19.92 (C-4′), 19.29 (C-3′, -5′); MS (ES+): *m*/*z* (%) 523 (20) ([2(M−Br)−1]$^+$), 262 (100) ([M−Br]$^+$); MS (EI) of salt **5** is identical to that of bromoalkyl derivative **7** arising from its thermal decomposition. Anal. Calcd for $C_{13}H_{16}BrN_3O_3$ (342.19): C 45.63; H 4.71; N 12.28. Found: C 45.50; H 4.87; N 12.52.

4.2.2.3. 4-Methyl-6-nitro-3-oxo-1,2,3,4-tetrahydroquinoxaline-1-spiro-1′-piperidinium bromide (6). Spiro chloride **4** (prepared[33] from 2,2′-dichloro-*N*-methyl-5′-nitroacetanilide and piperidine or by cyclization of 2-chloro-*N*-methyl analogue of **2**) (7.79 g, 25 mmol), treated with 48% aq hydrobromic acid as described for the preparation of salt **5**, afforded the title bromide **6** (7.93 g, 89% yield). Mp 159–162 °C (decomp.) (ethanol); ^{1}H NMR (DMSO-d_6): δ 8.34 (d, *J* = 9.0 Hz, 1H, 8-H), 8.23 (dd, *J* = 9.0, 2.4 Hz,1H, 7-H), 8.18 (d, *J* = 2.4 Hz, 1H, 5-H), 4.97 (s, 2H, 2-H), 4.14 (m, J_{gem} = (−)12.1 Hz, $J_{a,a}$ = 9.8 Hz, 2H, 2′-,6′-H$_a$), 3.90 (br d, J_{gem} = (−)12.1 Hz, 2H, 2′-,6′-H$_e$), 3.45 (s, 3H, 4-CH_3), 2.17 (m, 2H) and 1.93–1.51 (m, 4H) (3′-,4′-,5′-H); ^{13}C NMR (DMSO-d_6): δ 160.14 (C-3), 148.93 (C-6), 136.39, 135.34 (C-4a, -8a), 122.62 (C-8), 118.87 (C-7), 112.82 (C-5), 61.48 (C-2′, -6′), 55.18 (C-2), 29.69 (4-CH_3), 19.93 (C-4′), 19.32 (C-3′, -5′); MS (ES+): *m*/*z* (%) 633 (5) ([2 M−Br+2]$^+$), 631 (5) ([2 M−Br]$^+$), 276 (100) ([M−Br]$^+$); MS (EI) of salt **6** is identical to that of bromoalkyl derivative **8** arising from its thermal decomposition. Anal. Calcd for $C_{14}H_{18}BrN_3O_3$ (356.22): C 47.20; H 5.09; N 11.80. Found: C 47.48; H 4.87; N 11.62.

4.2.2.4. 4-(5-Bromopentyl)-7-nitro-3,4-dihydro-1*H*-quinoxalin-2-one (7). A suspension of bromide **5** (6.84 g, 20 mmol) in nitromethane (50 mL) was refluxed for 48 h under argon atmosphere. After cooling, the solid in suspension, collected by filtration,

washed with nitromethane (2 × 10 mL) and air-dried, was shown to be the bromopentyl derivative **7** (6.43 g, 94% yield). Similar results were obtained starting from bromoacetanilide **2**, following the same procedure but without isolation of the intermediate salt **5**. Mp 192–195 °C (decomp.) (nitromethane).^{1}H NMR (DMSO-d_6): δ 10.78 (s, 1H, 1-H), 7.77 (dd, J = 9.3, 2.7 Hz,1H, 6-H), 7.59 (d, J = 2.7 Hz, 1H, 8-H), 6.77 (d, J = 9.3 Hz, 1H, 5-H), 4.04 (s, 2H, 3-H), 3.53 (t, J = 6.7 Hz, 2H, 5′-H), 3.34 (t, J = 7.3 Hz, 2H, 1′-H), 1.84 (m, 2H, 4′-H), 1.59 (m, 2H, 2′-H), 1.42 (m, 2H, 3′-H); ^{13}C NMR (DMSO-d_6): δ 163.82 (C-2), 140.20 (C-4a), 136.46 (C-7), 125.57 (C-8a), 120.58 (C-6), 109.66 (C-8), 109.17 (C-5), 51.00 (C-3), 48.96 (C-1′), 35.00 (C-5′), 31.99 (C-24′), 24.92 (C-3′), 23.64 (C-2′); MS (EI): m/z (%) 343 (24) ([M+2]$^+$), 341 (24) (M$^+$), 262 (17), 206 (100), 178 (45), 160 (10), 132 (23), 118 (8). Anal. Calcd for $C_{13}H_{16}BrN_3O_3$ (342.19): C 45.63; H 4.71; N 12.28. Found: C 45.55; H 4.61; N 12.52.

4.2.2.5. 4-(5-Bromopentyl)-1-methyl-7-nitro-3,4-dihydro-1*H*-quinoxalin-2-one (8). A suspension of bromide **6** (7.12 g, 20 mmol) in nitromethane (50 mL) was refluxed for 24 h under argon. The solvent was then evaporated to dryness and the residue triturated with ethanol (20 mL); the insoluble material was collected by filtration, washed with cold ethanol (2 × 10 mL) and air-dried yielding compound **8** (5.91 g, 83% yield). Mp 118–120 °C (ethanol). ^{1}H NMR (DMSO-d_6): δ 7.88 (dd, J = 9.3, 2.4 Hz,1H, 6-H), 7.69 (d, J = 2.4 Hz, 1H, 8-H), 6.85 (d, J = 9.3 Hz, 1H, 5-H), 4.12 (s, 2H, 3-H), 3.53 (t, J = 6.7 Hz, 2H, 5′-H), 3.37 (t, J = 7.6 Hz, 2H, 1′-H), 3.32 (s, 3H, 1-CH_3), 1.84 (m, 2H, 4′-H), 1.58 (m, 2H, 2′-H), 1.43 (m, 2H, 3′-H; ^{13}C NMR (DMSO-d_6): δ 163.27 (C-2), 141.71 (C-4a), 136.85 (C-7), 127.64 (C-8a), 120.79 (C-6), 109.65, 109.51 (C-5, -8), 51.02 (C-3), 49.01 (C-1′), 34.94 (C-5′), 31.92 (C-4′), 28.25 (1-CH_3), 24.87 (C-3′), 23.57 (C-2′); MS (EI): m/z (%) 357 (33) ([M+2]$^+$), 355 (33) (M$^+$), 276 (17), 220 (100), 192 (72), 160 (7), 146 (29), 131 (12), 104 (5). Anal. Calcd for $C_{14}H_{18}BrN_3O_3$ (356.22): C 47.20; H 5.09; N 11.80. Found: C 47.48; H 5.19; N 11.62.

4.2.2.6. Preparation of 4-[5-(dialkylamino)pentyl]quinoxalin-2-ones hydrobromides 9–18. For dimethylamino derivatives **9** and **14**, the corresponding bromide (**7** or **8**) (3 mmol) and dimethylamine (7.5 mmol; 1.34 mL of a 5.6 M solution in ethanol) in 1,4-dioxane (100 mL) was heated in an autoclave at 100–110 °C until the starting bromide was consumed (ca. 6 h). For cyclic secondary amines derivatives **10**–**13** and **15**–**18**, a mixture of the corresponding bromide (**7** or **8**) (3 mmol) and the required amine (7.5 mmol) in 1,4-dioxane (100 mL) was refluxed until the starting bromide was consumed (5–10 h). After eventual separation (filtration or decantation), some tars appeared when using dimethylamine or pyrrolidine, dioxane was evaporated to dryness and ethanol (10 mL) and 48% aq hydrobromic acid (0.5 mL) were added. The mixture was stirred for 2 h and the precipitated hydrobromide collected by filtration, washed with ethanol (2 × 5 mL) and air-dried (83–98% yield).

4.2.2.7. 4-[5-(Dimethylamino)pentyl]-7-nitro-3,4-dihydro-1*H*-quinoxalin-2-one hydrobromide (9). Yield: 0.98 g (84%); mp 204–207 °C (methanol); ^{1}H NMR (DMSO-d_6): δ 10.81 (s, 1H, 1-H), 9.44 (br s, 1H, 5′-NH$^+$), 7.77 (dd, J = 9.3, 2.7 Hz,1H, 6-H), 7.60 (d, J = 2.7 Hz, 1H, 8-H), 6.80 (d, J = 9.3 Hz, 1H, 5-H), 4.06 (s, 2H, 3-H), 3.35 (t, J = 7.5 Hz, 2H, 1′-H), 3.03 (m, 2H, 5′-H), 2.75 [s, 6H, N(CH_3)$_2$], 1.61 (m, 4H, 2′-,4′-H), 1.33 (m, 2H, 3′-H); ^{13}C NMR (DMSO-d_6): δ 163.86 (C-2), 140.27 (C-4a), 136.43 (C-7), 125.59 (C-8a), 120.60 (C-6), 109.66, 109.30 (C-5, -8), 56.34 (C-5′), 51.08 (C-3), 48.84 (C-1′), 42.09 [N(CH_3)$_2$], 24.03, 23.44, 23.09 (C-2′, -3′, -4′). MS (ES+): m/z (%) 695 (12) ([2 M−Br+2]$^+$), 693 (12) ([2 M−Br]$^+$), 308 (20) ([M−Br+1]$^+$), 307 (100) ([M−Br]$^+$).Anal. Calcd for $C_{15}H_{23}BrN_4O_3$ (387.27): C 46.52; H 5.99; N 14.47. Found: C 46.50; H 5.77; N 14.21.

4.2.2.8. 7-Nitro-4-(5-pyrrolidinopentyl)-3,4-dihydro-1*H*-quinoxalin-2-one hydrobromide (10). Yield: 1.22 g (98%); mp 233–235 °C (decomp.) (water); ^{1}H NMR (DMSO-d_6): δ 10.81 (s, 1H, 1-H), 9.60 (br s, 1H, 1″-H), 7.77 (dd, J = 9.3, 2.7 Hz,1H, 6-H), 7.60 (d, J = 2.7 Hz, 1H, 8-H), 6.80 (d, J = 9.3 Hz, 1H, 5-H), 4.06 (s, 2H, 3-H), 3.49 (br s, 2H, 2″-,5″-H_A), 3.35 (t, J = 7.4 Hz, 2H, 1′-H), 3.10 (m, 2H, 5′-H), 2.97 (br s, 2H, 2″-,5″-H_B), 1.95 (br s, 2H) and 1.87 (br s, 2H) (3″-,4″-H), 1.63 (m, 4H, 2′-,4′-H), 1.33 (m, 2H, 3′-H). ^{13}C NMR (DMSO-d_6): δ 163.79 (C-2), 140.22 (C-4a), 136.38 (C-7), 125.54 (C-8a), 120.59 (C-6), 109.62, 109.29 (C-5, -8), 53.58 (C-5′), 52.94 (C-2″, -5″), 51.05 (C-3), 48.85 (C-1′), 24.85, 23.96, 23.23 (C-2′, -3′, -4′), 22.61 (C-3″, -4″).MS (ES+): m/z (%) 747 (14) ([2 M−Br+2]$^+$), 745 (13) ([2 M−Br]$^+$), 334 (23) ([M−Br+1]$^+$), 333 (100) ([M−Br]$^+$). Anal. Calcd for $C_{17}H_{25}BrN_4O_3$ (413.31): C 49.40; H 6.10; N 13.56. Found: C 49.50; H 6.37; N 13.72.

4.2.2.9. 7-Nitro-4-(5-piperidinopentyl)-3,4-dihydro-1*H*-quinoxalin-2-one hydrobromide (11). Yield: 1.24 g (97%); mp 246–248 °C (decomp.) (methanol); ^{1}H NMR (DMSO-d_6): δ 10.81 (s, 1H, 1-H), 9.08 (br s, 1H, 1″-H), 7.78 (dd, J = 9.0, 2.7 Hz,1H, 6-H), 7.60 (d, J = 2.7 Hz, 1H, 8-H), 6.80 (d, J = 9.0 Hz, 1H, 5-H), 4.06 (s, 2H, 3-H), 3.37 (m, 4H, 1′-H, 2″-,6″-H_e), 3.00 (m, 2H, 5′-H), 2.83 (m, 2H, 2″-,6″-H_a), 1.67 (m, 9H, 2′-,4′-,3″-,5″-H, 4″-H_A), 1.33 (m, 3H, 3′-H, 4″-H_B); ^{13}C NMR (DMSO-d_6): δ163.85 (C-2), 140.26 (C-4a), 136.43 (C-7), 125.59 (C-8a), 120.59 (C-6), 109.66, 109.28 (C-5, -8), 55.59 (C-5′), 51.95 (C-2″, -6″), 51.06 (C-3), 48.81 (C-1′), 24.02, 23.31, 22.93 (C-2′, -3′, -4′), 22.45 (C-3″, -5″), 21.34 (C-4″). MS (ES+): m/z (%) 775 (8) ([2 M−Br+2]$^+$), 773 (8) ([2 M−Br]$^+$), 348 (25) ([M−Br+1]$^+$), 347 (100) ([M−Br]$^+$). Anal. Calcd for $C_{18}H_{27}BrN_4O_3$ (427.34): C 50.59; H 6.37; N 13.11. Found: C 50.50; H 6.47; N 13.32.

4.2.2.10. 4-(5-Azepanylpentyl)-7-nitro-3,4-dihydro-1*H*-quinoxalin-2-one hydrobromide (12). Yield: 1.28 g (97%); mp 235–237 °C (decomp.) (methanol); ^{1}H NMR (DMSO-d_6): δ 10.82 (s, 1H, 1-H), 9.13 (br s, 1H, 1″-H), 7.79 (dd, J = 9.0, 2.7 Hz,1H, 6-H), 7.61 (d, J = 2.7 Hz, 1H, 8-H), 6.80 (d, J = 9.0 Hz, 1H, 5-H), 4.06 (s, 2H, 3-H), 3.35 (m, 4H, 1′-H, 2″-,7″-H_A), 3.06 (m, 4H, 5′-H, 2″-,7″-H_B), 1.90–1.50 (m, 12H, 2′-,4′-,3″-,4″-,5″-,6″-H), 1.33 (m, 2H, 3′-H); ^{13}C NMR (DMSO-d_6): δ 163.83 (C-2), 140.26 (C-4a), 136.42 (C-7), 125.58 (C-8a), 120.58 (C-6), 109.64, 109.27 (C-5, -8), 56.06 (C-5′), 53.53 (C-2″, -7″), 51.06 (C-3), 48.82 (C-1′), 25.94 (C-3″, -6″), 24.04, 23.32, 23.29 (C-2′, -3′, -4′), 22.86 (C-4″, -5″). MS (ES+): m/z (%) 803 (18) ([2 M−Br+2]$^+$), 801 (17) ([2 M−Br]$^+$), 362 (24) ([M−Br+1]$^+$), 361 (100) ([M−Br]$^+$). Anal. Calcd for $C_{19}H_{29}BrN_4O_3$ (441.36): C 51.70; H 6.62; N 12.69. Found: C 51.98; H 6.67; N 12.62.

4.2.2.11. 7-Nitro-4-[5-(1,2,3,4-tetrahydroisoquinolin-2-yl)pentyl]-3,4-dihydro-1*H*-quinoxalin-2-one hydrobromide (13) Yield: 1.34 g (94%); mp 196–198 °C (decomp.) (0.5 M aq HBr); ^{1}H NMR (DMSO-d_6): δ 10.83 (s, 1H, 1-H), 9.73 (br s, 1H, 2″-H), 7.79 (dd, J = 9.3, 2.7 Hz,1H, 6-H), 7.61 (d, J = 2.7 Hz, 1H, 8-H), 7.32-7.16 (m, 4H, 5″-,6″-,7″-,8″-H), 6.82 (d, J = 9.3 Hz, 1H, 5-H), 4.55 [br d, J = (−)15.3 Hz, 1″-H_A], 4.29 [br dd, J = (−)15.3, 8.3 Hz, 1″-H_B], 4.07 (s, 2H, 3-H), 3.70 (m, 1H, 3″-H_A), 3.35 (t, J = 7.2 Hz, 2H, 1′-H), 3.30–2.95 (m, 5H, 5′-,4″-H, 3″-H_B), 1.79 (m, 2H, 4′-H), 1.63 (m, 2H, 2′-H), 1.38 (m, 2H, 3′-H). ^{13}C NMR (DMSO-d_6): δ 163.73 (C-2), 140.19 (C-4a), 136.44 (C-7), 131.25, 128.48, 126.59, 126.55 (C-5″, -6″, -7″, -8″), 128.31, 127.64 (C-4″a, -8″a), 125.55 (C-8a), 120.48 (C-6), 109.62 (C-8), 109.25 (C-5),54.90 (C-5′),51.71 (C-1″), 51.05 (C-3), 48.81 (C-1′), 48.76 (C-3″), 24.78 (C-4″), 24.00 (C-2′), 23.21 (C-3′), 23.03 (C-4′). MS (ES+): m/z (%) 871 (6) ([2 M−Br+2]$^+$), 869 (6) ([2 M−Br]$^+$), 396 (28) ([M−Br+1]$^+$), 395 (100) ([M−Br]$^+$). Anal. Calcd for $C_{22}H_{27}BrN_4O_3$ (475.38): C 55.58; H 5.72; N 11.79. Found: C 55.50; H 5.67; N 11.52.

4.2.2.12. 4-[5-(Dimethylamino)pentyl]-1-methyl-7-nitro-3,4-dihydro-1*H*-quinoxalin-2-one hydrobromide (14). Yield: 1.00 g (83%); mp 182–184 °C (decomp.) (ethanol); ^{1}H NMR (DMSO-d_6): δ 9.38 (br s, 1H, 5′-NH$^+$), 7.88 (dd, J = 9.3, 2.4 Hz,1H, 6-H), 7.70 (d, J = 2.4 Hz, 1H, 8-H), 6.88 (d, J = 9.3 Hz, 1H, 5-H), 4.13 (s, 2H, 3-H), 3.38 (t, J = 7.1 Hz, 2H, 1′-H), 3.32 (s, 3H, 1-CH_3), 3.03 (m, 2H, 5′-H), 2.74 [s, 6H, N(CH_3)$_2$], 1.63 (m, 4H, 2′-,4′-H), 1.34 (m, 2H, 3′-H); ^{13}C NMR (DMSO-d_6): δ 163.35 (C-2), 141.81 (C-4a), 136.88 (C-7), 127.70 (C-8a), 120.85 (C-6), 109.78, 109.61 (C-5, -8), 56.35 (C-5′), 51.13 (C-3), 48.91 (C-1′), 42.10 [N(CH_3)$_2$], 28.30 (1-CH_3), 23.99, 23.42, 23.09 (C-2′, -3′, -4′); MS (ES+): m/z (%) 723 (8) ([2 M−Br+2]$^+$), 721 (8) ([2 M−Br]$^+$), 322 (20) ([M−Br+1]$^+$), 321 (100) ([M−Br]$^+$). Anal. Calcd for $C_{16}H_{25}BrN_4O_3$ (401.30): C 47.89; H 6.28; N 13.96. Found: C 47.64; H 6.47; N 13.92.

4.2.2.13. 1-Methyl-7-nitro-4-(5-pyrrolidinopentyl)-3,4-dihydro-1*H*-quinoxalin-2-one hydrobromide (15). Yield: 1.13 g (88%); mp 206–208 °C (decomp.) (ethanol).;^{1}H NMR (DMSO-d_6): δ 9.46 (br s, 1H, 1″-H), 7.90 (dd, J = 9.0, 2.4 Hz,1H, 6-H), 7.72 (d, J = 2.4 Hz, 1H, 8-H), 6.87 (d, J = 9.0 Hz, 1H, 5-H), 4.14 (s, 2H, 3-H), 3.50 (br s, 2H, 2″-,5″-H_A), 3.38 (t, J = 7.3 Hz, 2H, 1′-H), 3.33 (s, 3H, 1-CH_3), 3.10 (m, 2H, 5′-H), 2.96 (br s, 2H, 2″-,5″-H_B), 1.97 (br s, 2H) and 1.83 (br s, 2H) (3″-,4″-H), 1.61 (m, 4H, 2′-,4′-H), 1.35 (m, 2H, 3′-H).); ^{13}C NMR (DMSO-d_6): δ 163.34 (C-2), 141.79 (C-4a), 136.84 (C-7), 127.67 (C-8a), 120.87 (C-6), 109.76, 109.63 (C-5, -8), 53.62 (C-5′), 53.01 (C-2″, -5″), 51.12 (C-3), 48.94 (C-1′), 28.30 (1-CH_3), 24.88, 23.96, 23.24 (C-2′, -3′, -4′), 22.58 (C-3″, -4″); MS (ES+): m/z (%) 775 (15) ([2 M−Br+2]$^+$), 773 (15) ([2 M−Br]$^+$), 348 (24) ([M−Br+1]$^+$), 347 (100) ([M−Br]$^+$). Anal. Calcd for $C_{18}H_{27}BrN_4O_3$ (427.34): C 50.59; H 6.37; N 13.11. Found: C 50.33; H 6.61; N 13.33.

4.2.2.14. 1-Methyl-7-nitro-4-(5-piperidinopentyl)-3,4-dihydro-1*H*-quinoxalin-2-one hydrobromide (16). Yield: 1.24 g (94%); mp 214–216 °C (decomp.) (ethanol); ^{1}H NMR (DMSO-d_6): δ 9.24 (br s, 1H, 1″-H), 7.88 (dd, J = 9.3, 2.4 Hz,1H, 6-H), 7.69 (d, J = 2.4 Hz, 1H, 8-H), 6.88 (d, J = 9.3 Hz, 1H, 5-H), 4.13 (s, 2H, 3-H), 3.37 (m, 4H, 1′-H, 2″-,6″-H_e), 3.31 (s, 3H, 1-CH_3), 3.00 (m, 2H, 5′-H), 2.85 (m, 2H, 2″-,6″-H_a), 1.90-1.50 (m, 9H, 2′-,4′-,3″-,5″-H, 4″-H_A), 1.33 (m, 3H, 3′-H, 4″-H_B); ^{13}C NMR (DMSO-d_6): δ 163.34 (C-2), 141.79 (C-4a), 136.84 (C-7), 127.68 (C-8a), 120.87 (C-6), 109.76, 109.62 (C-5, -8), 55.58 (C-5′), 51.93 (C-2″, -6″), 51.12 (C-3), 48.91 (C-1′), 28.30 (1-CH_3), 23.96, 23.31, 22.89 (C-2′, -3′, -4′), 22.43 (C-3″, -5″), 21.34 (C-4″); MS (ES+): m/z (%) 803 (15) ([2 M−Br+2]$^+$), 801 (13) ([2 M−Br]$^+$), 362 (24) ([M−Br+1]$^+$), 361 (100) ([M-Br]$^+$). Anal. Calcd for $C_{19}H_{29}BrN_4O_3$ (441.36): C 51.70; H 6.62; N 12.69. Found: C 51.57; H 6.67; N 12.45.

4.2.2.15. 4-(5-Azepanylpentyl)-1-methyl-7-nitro-3,4-dihydro-1*H*-quinoxalin-2-one hydrobromide (17). Yield: 1.24 g (91%); mp 223–225 °C (decomp.) (ethanol); ^{1}H NMR (DMSO-d_6): δ 9.11 (br s, 1H, 1″-H), 7.90 (dd, J = 9.0, 2.6 Hz,1H, 6-H), 7.72 (d, J = 2.6 Hz, 1H, 8-H), 6.87 (d, J = 9.0 Hz, 1H, 5-H), 4.13 (s, 2H, 3-H), 3.39 (m, 4H, 1′-H, 2″-,7″-H_A), 3.33 (s, 3H, 1-CH_3), 3.06 (m, 4H, 5′-H, 2″-,7″-H_B), 1.90-1.50 (m, 12H, 2′-,4′-,3″-,4″-,5″-,6″-H), 1.33 (m, 2H, 3′-H); ^{13}C NMR (DMSO-d_6): δ 163.35 (C-2), 140.81 (C-4a), 136.87 (C-7), 127.70 (C-8a), 120.87 (C-6), 109.77, 109.62 (C-5, -8), 56.07 (C-5′), 53.57 (C-2″, -7″), 51.13 (C-3), 48.92 (C-1′), 28.30 (1-CH_3), 25.93 (C-3″, -6″), 24.01, 23.31 (2C) (C-2′, -3′, -4′), 22.89 (C-4″, -5″). MS (ES+): m/z (%) 831 (13) ([2 M−Br+2]$^+$), 829 (12) ([2 M−Br]$^+$), 376 (28) ([M−Br+1]$^+$), 375 (100) ([M−Br]$^+$). Anal. Calcd for $C_{20}H_{31}BrN_4O_3$ (455.39): C 52.75; H 6.86; N 12.30. Found: C 52.49; H 6.59; N 12.51.

4.2.2.16. 1-Methyl-7-nitro-4-[5-(1,2,3,4-tetrahydroisoquinolin-2-yl)pentyl]-3,4-dihydro-1*H*-quinoxalin-2-one hydrobromide (18). Yield: 1.29 g (88%); mp 184–187 °C (decomp.) (methanol); ^{1}H NMR (DMSO-d_6): δ 9.95 (br s, 1H, 2″-H), 7.89 (dd, J = 9.1, 2.4 Hz,1H, 6-H), 7.70 (d, J = 2.4 Hz, 1H, 8-H), 7.32-7.14 (m, 4H, 5″-,6″-,7″-,8″-H), 6.90 (d, J = 9.1 Hz, 1H, 5-H), 4.54 (br s, 1″-H_A), 4.34 (br s, 1″-H_B), 4.15 (s, 2H, 3-H), 3.71 (m, 1H, 3″-H_A), 3.41 (t, J = 7.1 Hz, 2H, 1′-H), 3.32 (s, 3H, 1-CH_3), 3.30-2.95 (m, 5H, 5′-, 4″-H, 3″-H_B), 1.83 (m, 2H, 4′-H), 1.63 (m, 2H, 2′-H), 1.40 (m, 2H, 3′-H). ^{13}C NMR (DMSO-d_6): δ 163.35 (C-2), 141.80 (C-4a), 136.86 (C-7), 131.31 (CH), 128.58 (CH), 128.41 (C_{ipso}), 127.74 (C_{ipso}), 127.68 (C_{ipso}), 126.68 (CH), 126.63 (CH) (C-8a, -4″a, -5″, -6″, -7″, -8″, -8″a), 120.88 (C-6),109.76 (C-8), 109.64 (C-5), 54.95 (C-5′), 51.81 (C-1″), 51.16 (C-3), 48.93 (C-1′), 48.85 (C-3″), 28.31 (1-CH_3), 24.87 (C-4″), 24.00 (C-2′), 23.26 (C-3′), 23.13 (C-4′). MS (ES+): m/z (%) 897 (7) ([2 M−Br+2]$^+$), 895 (7) ([2 M−Br]$^+$), 410 (29) ([M−Br+1]$^+$), 409 (100) ([M−Br]$^+$). Anal. Calcd for $C_{23}H_{29}BrN_4O_3$ (489.41): C 56.45; H 5.97; N 11.45. Found: C 56.57; H 6.21; N 11.69.

4.3. Wet evaluation: pharmacological assays

4.3.1. Determination of in vitro trichomonacidal activity

The biological activity was assayed on *Trichomonas vaginalis* JH31A #4 Ref. No. 30326 (ATCC, MD, USA) in modified Diamond medium supplemented with equine serum and grown at 37 °C (5% CO_2). The compounds were added to the cultures at several concentrations (100, 10, and 1 μg/mL) after 6 h of seeding (0 h). Viable protozoa were assessed at 24 and 48 h after incubation at 37 °C by using the Neubauer chamber. Metronidazole (Sigma-Aldrich SA, Spain) was used as a reference drug at concentrations of 2, 1, 0.5 μg/mL. Cytocidal and cytostatic activities were determined by calculation of percentages of cytocidal (%C) and cytostatic activities (%CA), in relation to controls as previously reported.[52]

4.3.2. *T. cruzi* epimastigote susceptibility assay

For this in vitro test,[25,53]the CL strain parasites (clone CL-B5) stably transfected with the *Escherichia coli* β-galactosidase gene (*LacZ*) were used. The epimastigotes were grown at 28 °C in liver infusion tryptose broth (LIT) with 10% foetal bovine serum (FBS), penicillin and streptomycin and harvested during the exponential growth phase. The screening assay was performed in 96-well microplates (Sarstedt, Sarstedt, Inc.) with cultures that had not reached the stationary phase. Briefly, epimastigotes form, CL strain, was seeded at concentration of 1×10^5 per milliliter in 200 μL media. The plates were then incubated at 28 °C for 72 h with various concentrations of the drugs (100, 10 and 1 μg/mL), at which time 50 μL of CPRG solution was added to give a final concentration of 200 μM. The plates were incubated at 37 °C for 6 hrs and the absorbances read at 595 nm. Each concentration was tested in triplicate and in order to avoid drawback, medium, negative and drug controls were used in each test. The anti-epimastigote percentage (%AE) was calculated as follows: %AE = [(AE − AEB)/(AC − ACB)] × 100, where AE = absorbance of experimental group; AEB = blank of compounds; AC = Absorbance of control group; ACB = blank of culture medium. Stock solutions of the compounds to be assayed were prepared in DMSO, with the final concentration in a water/DMSO mixture never exceeding 0.2% of the latter solvent.[25,53] Nifurtimox was used as reference drug.

4.3.3. In vitro cytotoxicity on macrophage cells

Murine J774 macrophages were grown in plastic 25 μL flasks in (RPMI)-1640 medium (Sigma) supplemented with 20% heat inactivated (30 min, 56 °C) foetal calf serum (FCS) and 100 IU penicillin/mL + 100 μg/mL streptomycin, in a humidified 5% CO_2/95% air atmosphere at 37 °C and subpassaged once a week. The J774 macrophages were seeded (70,000 cells/well) in 96-well flat-bottom microplates (Nunc) with 200 μL of medium. The cells were allowed to attach for 24 h at 37 °C and then exposed to the compounds (dissolved in DMSO, maximal final concentration of solvent was 0.2%) for another 24 h. Afterwards, the cells were washed with

PBS and incubated (37 °C) with 3-(4,5-dimethylthiazol-2-yl)-2,5-diphenyltetrazolium bromide (MTT) 0.4 mg/mL for 60 min. The MTT solution was removed and the cells solubilized in DMSO (10 μL). The extent of reduction of MTT to formazan within cells was quantified by measurement of OD595.[54] Each concentration was assayed three times and six cell growth controls were used in each test. The assays were performed in duplicate. Nifurtimox cytotoxicity was also determined. Cytotoxic percentages (%C) were determined as follows: $\%C = [1 - (ODp - ODpm)/(ODc - ODm)] \times 100$, where ODp represents the mean OD595 value recorded for wells with macrophages containing different doses of product; ODpm represents the mean OD595 value recorded for different concentrations of product in medium; ODc represents the mean OD595 value recorded for wells with macrophages and no product (growth controls), and ODm represents the mean OD595 value recorded for medium/control wells. The 50% cytotoxic dose (CD_{50}) was defined as the concentration of drug that decreases OD595 up to 50% of that in control cultures.[25]

4.3.4. *L. braziliensis* promastigotes susceptibility test

The tested chemicals were solubilized in DMSO (Sigma) to prepare a working solution of 10 mg/mL. Later on it was diluted in RPMI 1640 medium to the final highest concentration of DMSO on 1.5%, which was not toxic to the parasites.

In this study we used *L. braziliensis* (MHOM/PE/95/LQ2), which was isolated in the province of La Convención, Cuzco, Perú. Cultures were handled as previously described.[55] Promastigotes were adapted for culture in RPMI 1640 liquid medium (Gibco-BRL) supplemented with 20% heat inactivated fetal bovine serum, vitamins and amino acids, at 22 °C. Logarithm phase cultures of promastigotes were used for experimental purposes.

The inhibition of promastigotes growth in vitro was assessed by using a quantitative colorimetric assay with the oxidation–reduction indicator Alamar Blue® Assay.[56]Briefly, promastigotes were serially diluted in 200 μL RPMI 1640 medium without phenol red and supplemented with 20% heat-inactivated fetal bovine serum in 96-well plates. To these wells were added parasites (106/well), and the drug concentration to be tested. After addition of 10% of Alamar Blue®, the plates were incubated at 22 °C. After 72 h, the plates were analyzed on a Microplate Reader Model 680 (Biorad, Hercules, CA) by using a test wavelength of 570 nm and a reference wavelength of 630 nm. The 50% inhibitory concentrations (IC_{50}) were calculated by linear regression analysis with 95% confidence limits. All experiments were performed three times each in duplicate, and the mean values were also calculated. A paired two-tailed *t*-test was used for analysis of the data. Values of $p < 0.05$ were considered significant.

4.3.5. In vitro efficacy studies with *Toxoplasma gondii* tachyzoites

The efficacy of chemicals was tested against tachyzoites form of *Toxoplasma gondii*.[44,45] Tachyzoites (1×10^6)weresettled in ependorf microtubes (500 μL, Axygen Scientific), and exposed to compounds **9**–**18** for four hours at room temperature in order to evaluate the viability of the parasites. One hundred and fifty tachyzoites were counted and the viability percentage was taken with trypan blue exclusion method by counting the number of living tachyzoites.

All chemicals were first dissolved in dimethyl sulfoxide [DMSO, sigma, 99.5% (GC)], and then diluted in BME (basal medium eagle) Sigma-Aldrich. The compounds were assayed in the range of 1 mM, 500 μM, 200 μM, 100 μM. The final concentration of DMSO did not exceed 0.2% which caused no damage to the parasite. Later, Balb c mice were used for parasite infections maintained in an animal facility with regulated environmental conditions of temperature, humidity and filtered air. Management was performed according to the country official norm NOM-062-ZOO-1999 for the production, care and use of laboratory animals (Mexico). *Toxoplasma* RH strain tachyzoites-were maintained by ip passages in female Balb/c mice. After cervical dislocation, parasites were recovered from i.p. exudates after a peritoneal washing with PBS (138 mM NaCl, 1.1 mM K_2PO_4, 0.1 mM Na_2HPO_4 and 2.7 mM KCl, pH7.2) and purified by filtration through 5 μm pore polycarbonate membranes (Millipore Co, Bedford, MN).[44,45]

For the study of the effect of the compounds on viabilit of *T. gondii*, 1×10^6 tachyzoites were incubated in ependorff tubes with the various concentrations of the VAM2 drugs in a total volume of 500 μL during different period of times. Maximal time evaluated was 4 h of drug exposure. VAM2 compounds were dissolved in dimethyl sulfoxide (DMSO) and then diluted to the respective concentration in MEM culture media without foetal calf serum and maintained at room temperature until its use. Fresh solutions were prepared the same day of the assay. After drug exposure, tachyzoites were incubated with 0.4% blue trypan dye (Gybco, BRL, Life Technologies, Grand Island NY) in PBS and immediately mounted in slides to be counted through an Axioscope 2 MOT/Plus (Carl Zeiss, Mexico). Negative controls consisted in tachyzoites incubated with MEM containing the equivalent concentrations of DMSO used for the dissolution of the several drug concentrations. An additional negative control included tachyzoites maintained in MEM throughout the assay, maximal time four hours. Percentage of viability was determined by counting the number of live parasites that excluded the dye in triplicate and by counting at least 500 parasites in each assay.[44,45]

4.3.6. Ferriprotoporphyrin (FP) IX biocrystallization inhibition test (FBIT)

The procedure for testing FP biocrystallization was performed according to the method of Deharo et al.[46] In a normal non-sterile flat bottom 96-well plate at 37 °C for 18–24 h it was placed a mixture containing either 50 μL of drug solution (from 5 to 0.0125 mg/mL) or 50 μL of solvent (for control), 50 μL of 0.5 mg/mL of haemin chloride (Sigma H 5533) freshly dissolved in DMSO and 100 μL of 0.5 M sodium acetate buffer pH 4.4. The final pH of the mixture was in the range 5–5.2. The following order of addition was followed: first the haemin chloride solution, second the buffer, and finally the solvent or the solution of drug. The plate was then centrifuged at 1600 *g* for 5 min. The supernatant was discarded by vigorously flipping of the plate upside down the plate twice. The remaining pellet was resuspended with 200 μL of DMSO to remove unreacted FP. The plate was then centrifuged once again and the supernatant similarly discarded. The pellet, consisting of precipitate of β-hematin, was dissolved in 150 μL of 0.1 M NaOH for direct (in the same plate) spectroscopic quantification at 405 nm with a micro-ELISA (Enzyme-Linked Immunosorbent Assay) reader (Titertek Multiskan MCC/340). The percentage of inhibition of FP biocrystallization was calculated as follows: $\text{Inhibition}(\%) = 100 \times [(\text{O.D. control} - \text{O.D. drug})/\text{O.D. control}]$, where O.D. represents the mean optical density for either controls or drugs.[24,46]The IC_{50} values were determined using the *TREND* function of the ExcelSoftware.

4.3.7. Assessment of antimalarial activity in vitro by a semiautomated microdilution technique

A rapid, semiautomated microdilution method was developed for measuring the activity of potential antimalarial drugs against cultured intraerythrocytic asexual forms of the human malaria parasite *Plasmodium falciparum*.[47]Microtitration plates were used to prepare serial dilutions of the compounds to be tested. Parasites (strain 3D7), obtained from continuous stock cultures, were subcultured in these plates for 42 h. Inhibition of uptake of a radiolabeled nucleic acid precursor by the parasites served as the

indicator of antimalarial activity.[47] Chloroquine was used as antimalarial reference drug in this assay.

Acknowledgments

One of the authors (M.-P. Y) thanks the program '*Estades Temporals per a Investigadors Convidats*' for a fellowship to work at Valencia University (2013).This work was supported in part by VLIR (Vlaamse InterUniversitaire Raad, Flemish Interuniversity Council, Belgium) under the IUC Program VLIR-UCLV. N.R. was supported by fellowship from CONACYT (Apoyos Integrales para la Formación de Doctores en Ciencias) and DGAPA (PROFIP) UNAM (México). We are grateful to CONACYT (México) for the grant No. 60864 (to R.M.) which partly supported the antitoxoplasma study. Marrero-Ponce, Y. thanks to the program '*International Professor*' for a fellowship to work at Cartagena University in 2013–2014.Last, but not least, the authors acknowledge also the partial financial support from Spanish '*Comisión Interministerial de Ciencia y Tecnología*' (CICYT) (Project reference: SAF2009-10399).

Supplementary data

Supplementary data (The complete list of compounds used in training and test sets, their a posteriori classification according to obtained models as well as other biological details.) associated with this article can be found, in the online version, at http://dx.doi.org/10.1016/j.bmc.2014.01.036. These data include MOL files and InChiKeys of the most important compounds described in this article.

References and notes

1. Ridley, R. G. *Nature* **2002**, *415*, 686.
2. Baneth, G.; Shawb, S. E. *Vet. Parasitol.* **2002**, *106*, 315.
3. Dardonville, C.; Brun, R. *J. Med. Chem.* **2004**, *47*, 2296.
4. Roldos, V.; Nakayama, H.; Rolón, M.; Montero-Torres, A.; Trucco, F.; Torres, S.; Vega, M. V.; Marrero-Ponce, Y.; Heguaburu, V.; Yaluff, G.; Gómez-Barrio, A.; Sanabria, L.; Ferreira, M. E.; de Arias, M. A.; Pandolfi, E. *Eur. J. Med. Chem.* **2007**. http://dx.doi.org/10.1016/j.ejmech.2007.11.007.
5. Gardner, T. B.; Hill, D. R. Clinic *Microbiol. Rev.* **2001**, *14*, 114.
6. Jarroll, E. L.; Sener, K. *Drug Res. Updat.* **2003**, *6*, 239.
7. Chavalitshewinkoon-Petmitr, P.; Ramdja, M.; Kajorndechakiat, S.; Ralph, R. K.; Denny, W. A.; Wilairat, P. *J. Antimicrob. Chem.* **2003**, *52*, 287.
8. Zuther, E.; Johnson, J. J.; Haselkorn, R.; McLeod, R.; Gornicki, P. *Proc. Natl. Acad. Sci. U.S.A.* **1999**, *96*, 13387.
9. Renslo, A. R.; McKerrow, J. H. *Nat. Chem. Biol.* **2006**, *2*, 701.
10. Mackey, Z. B.; Baca, A. M.; Mallari, J. P.; Apsel, B.; Shelat, A.; Hansell, E. J.; Chiang, P. K.; Wolff, B. W.; Guy, K. R.; Williams, J.; McKerrow, J. H. *Chem. Biol. Drug Des.* **2006**, *67*, 355.
11. St. George, S.; Bishop, J. V.; Titus, R. G.; Selitrennikoff, C. P. *Antimicrob. Agents Chemother.* **2006**, *50*, 474.
12. Weisman, J. L.; Liou, A. P.; Shelat, A. A.; Cohen, F. E.; Guy, R. K.; DeRisi, J. L. *Chem. Biol. Drug Des.* **2006**, *67*, 409.
13. Chong, C. R.; Chen, X.; Shi, L.; Liu, J. O.; Sullivan, D. J. *Nat. Chem. Biol.* **2006**, *2*, 415.
14. Marrero-Ponce, Y.; Romero, V.; Central University of Las Villas: Santa Clara, Villa Clara, 2002.
15. Marrero-Ponce, Y. *Bioorg. Med. Chem.* **2004**, *12*, 6351.
16. Marrero Ponce, Y. *J. Chem. Inf. Comput. Sci.* **2004**, *44*, 2010.
17. Marrero-Ponce, Y.; Huesca-Guillen, A.; Ibarra-Velarde, F. *J. Mol. Struct. (Theochem)* **2005**, *717*, 67.
18. Marrero-Ponce, Y.; Torrens, F.; García-Domenech, R.; Ortega-Broche, S. E.; Romero Zaldivar, V. *J. Math. Chem.* **2008**. http://dx.doi.org/10.1007/s10910.
19. Marrero-Ponce, Y.; Meneses-Marcel, A.; Catillo-Garit, J. A.; Machado-Tugores, Y.; Escario, J. A.; Gómez-Barrio, A.; Montero Pereira, D.; Nogal-Ruiz, J. J.; Arán, V. J.; Martínez-Fernández, A. R.; Torrens, F.; Rotondo, R. *Bioorg. Med. Chem.* **2006**, *14*, 6502.
20. Meneses-Marcel, A.; Marrero-Ponce, Y.; Machado-Tugores, Y.; Montero-Torres, A.; Montero Pereira, D.; Escario, J. A.; Nogal-Ruiz, J. J.; Ochoa, C.; Arán, V. J.; Martínez-Fernández, A. R.; García Sánchez, R. N. *Bioorg. Med. Chem. Lett.* **2005**, *17*, 3838.
21. Rivera-Borroto, O. M.; Marrero-Ponce, Y.; Meneses-Marcel, A.; Escario, J. A.; Gómez-Barrio, A.; Arán, V. J.; Martins-Alho, M. A.; Montero Pereira, D.; Nogal, J. J.; Torrens, F.; Ibarra-Velarde, F.; Vera Montenegro, V.; Huesca-Guille, A.; Rivera, N.; Vogel, V. *QSAR Comb. Sci.* **2008**. http://dx.doi.org/10.1002/qsar.200610165.
22. Marrero-Ponce, Y.; Castillo-Garit, J. A.; Olazabal, E.; Serrano, H. S.; Morales, A.; Castanedo, N.; Ibarra-Velarde, F.; Huesca-Guillen, A.; Sanchez, A. M.; Torrens, F.; Castro, E. A. *Bioorg. Med. Chem.* **2005**, *13*, 1005.
23. Marrero-Ponce, Y.; Iyarreta-Veitia, M.; Montero-Torres, A.; Romero-Zaldivar, C.; Brandt, C. A.; Avila, P. E.; Kirchgatter, K.; Machado, Y. *J. Chem. Inf. Comput. Sci.* **2005**, *45*, 1082.
24. Montero-Torres, A.; García-Sánchez, R. N.; Marrero-Ponce, Y.; Machado-Tugores, Y.; Nogal-Ruiz, J. J.; Martínez-Fernández, A. R.; Arán, V. J.; Ochoa, C.; Meneses-Marcel, A.; Torrens, F. *Eur. J. Med. Chem.* **2006**, *41*, 483.
25. Vega, M. C.; Montero-Torres, A.; Marrero-Ponce, Y.; Rolón, M.; Gómez-Barrio, A.; Escario, J. A.; Arán, V. J.; Martínez-Fernández, A. R.; Meneses-Marcel, A. *Bioorg. Med. Chem. Lett.* **2006**, *16*, 1898.
26. Montero-Torres, A.; Vega, M. C.; Marrero-Ponce, Y.; Rolón, M.; Gómez-Barrio, A.; Escario, J. A.; Arán, V. J.; Martínez-Fernández, A. R.; Meneses-Marcel, A. *Bioorg. Med. Chem.* **2005**, *13*, 6264.
27. Arán, V. J.; Asensio, J. L.; Ruiz, J. R.; Stud, M. *J. Chem. Soc., Perkin Trans. 1* **1993**, 1119.
28. Arán, V. J.; Flores, M.; Muñoz, M.; Ruiz, J. R.; Sánchez-Verdú, P.; Stud, M. *Liebigs Ann.* **1995**, 817.
29. Arán, V. J.; Flores, M.; Muñoz, M.; Páez, J. A.; Sánchez-Verdú, P.; Stud, M. *Liebigs Ann.* **1996**, 683.
30. Arán, V. J.; Ochoa, C.; Boiani, L.; Buccino, P.; Cerecetto, H.; Gerpe, A.; Gonzalez, M.; Montero, D.; Nogal, J. J.; Gomez-Barrio, A.; Azqueta, A.; Lopez de Cerain, A.; Piro, O. E.; Castellano, E. E. *Bioorg. Med. Chem.* **2005**, *13*, 3197.
31. Ruiz, J. R.; Arán, V. J.; Asensio, J. L.; Flores, M.; Stud, M. *Liebigs Ann. Chem.* **1994**, 679.
32. Arán, V. J.; Asensio, J. L.; Molina, J.; Muñoz, P.; Ruiz, J. R.; Stud, M. *J. Chem. Soc., Perkin Trans. 1* **1997**, 2229.
33. de Castro, S.; Chicharro, R.; Arán, V. J. *J. Chem. Soc., Perkin Trans. 1* **2002**, 790.
34. Marrero-Ponce, Y.; Montero-Torres, A.; Zaldivar, C. R.; Veitia, M. I.; Perez, M. M.; Sanchez, R. N. *Bioorg. Med. Chem.* **2005**, *13*, 1293.
35. Nwaka, S.; Besson, D.; Ramirez, B.; Maes, L.; Matheeussen, A.; Bickle, Q.; Mansour, N. R.; Yousif, F.; Townson, S.; Gokool, S.; Cho-Ngwa, F.; Samje, M.; Misra-Bhattacharya, S.; Murthy, P. K.; Fakorede, F.; Paris, J.-M.; Yeates, C.; Ridley, R.; Voorhis, W. C. V.; Geary, T. *PLoS Negl. Trop Dis.* **2011**, *5*, 1412.
36. OECD. In *OECD Environment Health and Safety Publication, Series on Testing and Assessment No. 69*: Paris, 2007. http://www.oecd.org/dataoecd/55/35/38130292.pdf.
37. Negwer, M. *Organic-Chemical Drugs and their Synonyms*; Akademie: Berlin, 1987.
38. Chapman and Hall, 1996.
39. Marrero-Ponce, Y.; Marrero, R. M.; Torrens, F.; Martinez, Y.; Bernal, M. G.; Zaldivar, V. R.; Castro, E. A.; Abalo, R. G. *J. Mol. Model.* **2005**, 1.
40. Gramatica, P. *QSAR Comb. Sci.* **2007**, *26*, 694.
41. Atkinson, A. C. *Plots, Transformations and Regression*; Clarendon Press: Oxford, 1985.
42. Papa, E.; Villa, F.; Gramatica, P. *J. Chem. Inf. Model.* **2005**, *45*, 1256.
43. Papageorgiou, J. G.; Yakob, L.; Al Salabi, M. L.; Diallinas, G.; Diallinas, G.; Soteriadou, K. P.; De Koning, H. P. *Parasitology* **2005**, *130*, 275.
44. Mondragón, R.; Frixione, E. *J. Eur. Microbiol.* **1996**, *43*, 120.
45. Patrón, A.; Mondragón, M.; Gonzáles, S.; Ambrosio, J.; Guerrero, A.; Mondragón, R. *Int. J. Parasitol.* **2005**, *35*, 883.
46. Deharo, E.; Garcia, R.; Oporto, P.; Sauvain, M.; Gautret, P.; Ginsburg, H. *Exp. Parasitol.* **2002**, *100*, 252.
47. Desjardins, R. E.; Canfield, C. J.; Haynes, J. D.; Chulay, J. D. *Antimicrob. Agents Chemother.* **1979**, *16*, 710.
48. Aguilera-Venegas, B.; Olea-Azar, C.; Norambuen, E.; Arán, V. J.; Mendizábal, F.; Lapier, M.; Maya, J. D.; Kemmerling, U.; López-Muñoz, R. *Spectrochim. Acta Part A* **2011**, *78*, 1004.
49. StatSoft Inc.: Tulsa, OK, 2001.
50. Baldi, A.; Dragonetti, E.; Battista, T.; Groeger, A. M.; Esposito, V.; Baldi, G.; Santini, D. *Anticancer Res.* **2000**, *20*, 3923.
51. Consonni, V.; Todeschini, R.; Pavan, M. *J. Chem. Inf. Comput. Sci.* **2002**, *42*, 682.
52. Kouznetsov, V. V.; Rivero, C. J.; Ochoa, P. C.; Stashenko, E.; Martínez, J. R.; Montero, P. D.; Nogal, R. J. J.; Fernández, P. C.; Muelas, S. S.; Gómez, B. A.; Bahsas, A.; Amaro, L. *J. Arch. Pharm. (Weinheim, Ger.)* **2005**, *338*, 32.
53. Vega, M. C.; Rolon, M.; Martinez-Fernandez, A. R.; Escario, J. A.; Gomez-Barrio, A. *Parasitol. Res.* **2005**, *95*, 296.
54. Hattori, Y.; Nakanishi, N. *Cell. Immunol.* **1995**, *165*, 7.
55. Piñero, J.; Temporal, R. M.; Silva-Goncalves, A. J.; Jimenez, I. A.; Bazzocchi, I. L.; Oliva, A.; Perer, A.; Leon, L. L.; Valladares, B. *Acta Trop.* **2006**, *98*, 59.
56. Cabrera-Serra, M. G.; Lorenzo-Morales, J.; Romero, M.; Valladares, B.; Piñero, J. *Parasitol. Res.* **2007**, *100*, 1155.